Impacts of upland open drains upon runoff generation: a numerical assessment of catchment-scale impacts

Stuart N. Lane (1) and David G. Milledge (2)

(1) Faculté des géosciences et de l'environnement, Université de Lausanne, LAUSANNE, CH-1015, Switzerland
(2) Department of Geography, Durham University, DURHAM, DH1 3LE, U.K.

Abstract

Shallow upland drains, grips, have been hypothesized as responsible for increased downstream flow magnitudes. Observations provide counterfactual evidence, often relating to the difficulty of inferring conclusions from statistical correlation and paired catchment comparisons; and the complexity of designing field experiments to test grip impacts at the catchment-scale. Drainage should provide drier antecedent moisture conditions, providing more storage at the start of an event; but, grips have higher flow velocities than overland flow so potentially delivering flow more rapidly to the drainage network. We develop and apply a model for assessing the impacts of grips upon flow hydrographs. The model was calibrated on the gripped case; then the gripped case was compared with the intact case by removing all grips. This comparison showed that even given parameter uncertainty, the intact case had significantly higher flood peaks and lower baseflows, mirroring field observations of the hydrological response of intact peat. The simulations suggest that this is because delivery effects may not to translate into catchment-scale impacts for three reasons. First, in our case, the proportions of flow path lengths that were hillslope were not changed significantly by gripping. Second, the structure of the grip network as compared with the structure of the drainage basin mitigated against grip-related increases in the concentration of runoff in the drainage network, although it did marginally reduce the mean timing of that concentration at the catchment outlet. Third, the effect of the latter upon downstream flow magnitudes can only be assessed by reference to the peak timing of other tributary basins, emphasizing that drain effects are both relative and scale dependent. However, given the importance of hillslope flow paths, we show that if upland drainage causes significant changes in surface roughness on hillslopes, then critical and important feedbacks may impact upon the speed of hydrological response.

Keywords
Flood risk; Peak flow; grips; drainage; uplands; peatlands; grip blocking

Introduction

It is not surprising that when faced with the need to increase economic productivity, conversion of peatlands through drainage was a commonly adopted measure, to allow the expansion of arable agriculture in lowlands, to prepare land for afforestation and to convert peat moorland to land more suitable for grazing. Thus, Holden *et al.* (2004) report extensive drainage in New Zealand, the Netherlands, Finland, Russia, Ireland and the U.K. In the U.K., economic subsidies and incentives for land drainage resulted in rates of drainage of over 100,000 ha per year in the early 1970s (Robinson and Armstrong, 1988) and by the early 1980s over 1.5 million hectares of blanket peat bog had been drained in the U.K. uplands (Stewart and Lance, 1983). These open cut drains (known as grips) are typically dug to around 0.5 m depth and 0.5 m width and laid out in a herring-bone pattern with short lateral ditches 5 - 50 m apart running sub-parallel to the slope contour and feeding into a central ditch (Holden *et al.*, 2004).

Holden *et al.* (2004) provide a detailed review of the debate over the hydrological impacts of grips. The debate has two elements, and each element has contrasting impacts (e.g. Ballard *et al.*, 2011). The first element relates to the effects of peatland drainage upon soil moisture characteristics, which have the potential to impact upon both high flows and low flows. Water balance calculations (e.g. Conway and Millar, 1960) have shown that an undrained upland hillslope could retain more water than a drained hillslope. Burke (1967) found for Glenamoy peats in Ireland that because the water table was generally high, undrained hillslopes tended to produce rapid runoff more rapidly during storm events. Subsequent research suggested that both of these processes can co-exist given the differences between the studies in their: antecedent conditions, peat type (e.g. McDonald, 1973), drainage density (e.g. Robinson, 1980, 1985) and interactions between these variables (e.g. in some peats, the effects of a drain may be laterally restricted (Stewart and Lance, 1991)). It is now generally recognized that peat produces rapid runoff from near-saturated slopes and relatively low base flows (Burt *et al.*, 1997; Evans *et al.*, 1999; Holden *et al.*, 2004; Ramchunder *et al.*, 2009). In fact, drained conditions would lead to a rapid increase in mineralization rates of organic matter and eventual peat decay. Drains act to reduce water table height in two ways. First, by creating a hydraulic gradient to draw water into the drain, producing water tables that are evenly drawn-down on either side of a drain (Dunn and Mackay, 1996). However, the saturated hydraulic conductivity of peat is so low that any localised drawdown towards the drain is likely to be limited to within 1-2 m of the drain itself (Stewart and Lance, 1991; Holden and Burt, 2003a; Holden et al., 2006b). Second, by redirecting upslope flows into the drain, reducing the contributing area downslope of the drain (Holden et al., 2006b; 2011). Thus, as a working hypothesis, through changes in moisture deficits, upland drainage should reduce peak flow by reducing the probability of saturation at the onset of a storm event; and increase baseflow by improving the ease with which the peat is able to drain during periods of low rainfall.

The second element of the effects of grips relates to their impacts upon the transfer of overland flow to the river network. This has been less well investigated through studies of water balance (Holden *et al.*, 2004). In theory, velocities in a newly drained or actively maintained grip (i.e. before revegetation) should be between one and two orders of magnitude greater than velocities over the hillslope or associated with rapid subsurface processes due to differences in surface roughness (Holden *et al.*, 2006). Provided that the grip does not increase the total flow path length, which would counter the effects of increased velocity, then this should deliver runoff more rapidly to the river network and so potentially increase flood peaks.

A series of studies have proposed that grips could increase flood peaks (e.g. Lewis, 1957; Oliver, 1958; Howe and Rodda, 1960; Conway and Miller, 1960; Ahti, 1980; Robinson, 1986; Guertin *et al.*, 1987; Gunn and Walker, 2000). Others have suggested that grips may reduce flood peaks (e.g. Burke, 1967; Baden and Egglesman, 1970; Newson and Robinson, 1983).

These studies are predominantly based upon either observing statistical changes in flood characteristics before and after the land management change, or upon paired catchment comparisons. Many fewer have instrumented catchments pre-drainage, during drainage and after drainage to assess drain impacts (Holden, *et al.*, 2004). Such studies are difficult because of the need for years or even decades, of instrumentation in order to characterize the baseline against which changes might be assessed given natural environmental variability. Further, it is quite possible that these contrasting conclusions are not entirely irresolvable, primarily because the magnitude of a flood peak depends upon the relative timing of the delivery of overland flow to the drainage network from each of the contributing areas. Changing the timing of delivery from one contributing area may increase or decrease downstream flood risk according to how the changed timing interacts with other contributing areas. Designing field experiments to assess these kinds of interactions is exceptionally difficult not least because of the huge numbers of combinations of grip effects that remain to be assessed. Thus, there is a second hypothesis for testing; that grips increase the speed of delivery of runoff to the channel network in ways that increase flood risk downstream.

Extremely few studies have explicitly recognized that grips may lead to the competing interaction of these two hypotheses (but see Holden *et al.*, 2006). The main exception to this is Wilson *et al.* (2010) who studied the effects of grip blocking. They found that blocking, quite rapidly, resulted in more seasonally stable and marginally higher water tables, certainly sufficient to increase the generation of saturation overland flow. However, albeit for only a very small catchment (12.5 Ha), they suggest that the rate of response of the catchment to rainfall was reduced, observing decreases in the 1 percentile excedance flow, based upon one year of data pre blocking and one year of data post blocking. They attributed the reduction in rate of response to a net effect of a reduced drainage density, the second hypothesis, notwithstanding the observation of higher water tables, the first hypothesis.

A critical issue runs through the literature relating to grip impacts: the difficulty of inferring conclusions from statistical correlation and paired catchment comparisons; and the complexity of designing field experiments that can test multiple possible grip scenarios at the catchment-scale. Recent developments in modeling are beginning to provide an alternative. Ballard *et al.* (2009, 2011, in press) report a quasi-3D, physically-based model, which couples three one-dimension models, one for each of subsurface, overland and channel flow, and apply it to test the effects of grip blocking over a 200 m x 200 m area (0.04 km^2). With this model, they were able to show the importance of grip spacing, surface roughness and channel roughness for hydrological response. However, their model does not upscale their results to entire catchments. In this paper, we aim to develop and to apply a model that is parsimonious with data typically available at the catchment scale and then to use it to test the differences in hydrograph characteristics with and without grips for a 13.8 km^2 catchment. Given the difficulties of adequately specifying the spatially-distributed characteristics (e.g. soil depth, hydraulic conductivity) of even a small upland catchment, we include in the methodology an explicit analysis of uncertainty.

Model Development

There are two critical elements of process representation required in the model. First, it must represent the effects of grips upon moisture deficits. Strictly, this requires a full three-dimensional solution of the shallow water equations for porous media (especially in peat soils). However, such a solution would not produce a model parsimonious with available boundary conditions (e.g. soil depth), initial conditions (e.g. soil wetness patterns), or parameterisation data. Hence, we chose to use the Network Index version of Topmodel (Lane *et al.,* 2004), as a model that had sufficient process complexity to capture grip impacts on moisture dynamics and runoff delivery but still allow us to undertake many 1000s of model runs so as to explore the effects of model uncertainty. We recognize two forms of model uncertainty in our analysis: (1) the more commonly explored effects of parameter uncertainty; and (2) the less frequently considered effects of choice of model structure, an issue that may impact also upon the level of parameter uncertainty. Second, in order to capture the effects of the drain network upon the timing of water delivery we also needed to modify Topmodel to represent, explicitly, flow routing over the hillslopes and through the network. This is explained below.

The basis of Topmodel is well rehearsed (e.g. Beven and Kirkby, 1979; Beven, 1997; Beven and Freer, 2001), and so the following section is brief. Topmodel partitions rainfall between three components: (1) overland flow (Q_o); (2) recharge of the unsaturated zone; and (3) flow in the saturated zone (Q_b). In simple terms, rain that falls on a unit of the landscape is assumed to go into storage in the unsaturated zone. If the soil is saturated, there is no recharge and the rainfall enters the channel network as overland flow, with an appropriate delay function (Beven and Kirkby, 1979). There is also flow within the saturated zone, which is estimated making two important assumptions (Beven and Kirkby, 1979): (1) runoff in the saturated zone is spatially uniform; and (2) the hydraulic gradient within the saturated zone is approximated by the local topographic slope, $\tan\beta$, requiring topographic data of sufficient resolution to allow an adequate description of the flow pathways without violating the assumption of local parallelism of the water table and soil surface (Saulnier, *et al.*, 1997).

In the standard Topmodel, it is assumed that the soil transmissivity function is an exponential function of storage deficit (Beven and Kirkby, 1979), of a shape controlled by a 'soil parameter' *m*, which is constant within each hydrological unit, and a transmissivity (T_o) at saturation (i.e. with zero deficit when the soil is saturated to the surface) which may vary locally but is also commonly held constant for each hydrological unit. Under this scenario, the local propensity to saturation is controlled by the topographic index: $\ln(a/\tan\beta)$; and the transmissivity. It is then possible to determine the saturated zone flux or base flow contribution (Q_b, mhr^{-1}) for each sub-unit of the catchment as well as the rate of recharge to the saturated zone from the unsaturated zone (Q_v) (e.g. Beven and Wood, 1983). Within this system, moisture accounting is treated in a lumped fashion for hydrologically similar areas: Q_b and Q_v are calculated for each time step; and then, in order to account for all rain that falls on a given catchment, the average catchment storage deficit ($\overline{D}_t$) is updated:

$$\overline{D}_t = \overline{D}_{t-1} + \frac{\Delta t}{A}\left(Q_b - Q_v\right)_{t-1} \quad [1]$$

where *t* is time. Although [1] is a lumped accounting model, for a given average catchment storage deficit it is possible to determine the critical value of the topographic index above which a location within the catchment will be saturated. Thus, it is possible to map the lumped predictions of storage deficit back onto a distributed map of locations where the saturation deficit is locally zero or negative and overland flow is likely to be occurring.

When the lumped predictions of storage deficit are mapped back onto catchment topographic data a basic component of Topmodel's process conceptualization is violated (Lane *et al.*, 2004): a distinction can be made between saturated areas that expand out of and back into the drainage network during the onset and end of a storm event; and saturated areas that remain entirely disconnected by overland flow for some or all of the event. Lane *et al.* (2004) attribute this to both a methodological difficulty associated with the effects of data uncertainty upon the propensity to create artificial pits on the catchment surface but also a substantive process where saturated areas can develop without being connected to the channel network. Assuming that such areas can contribute runoff when disconnected may lead to them contributing runoff too quickly. It will also change the rate at which the catchment becomes saturated (following from [1]) as unconnected saturated areas are assumed to contribute to overland flow when water might otherwise re-infiltrate in zones of lower topographic index before the channel is reached.

To deal with this problem, Lane *et al.* (2004) propose the Network Index modification of Topmodel. The basic principle of the network index approach is straightforward: a saturated area can only connect to the drainage network when all cells in the model between the saturated area and the network are themselves saturated. Lane *et al.* (2009) tested the Network Index as an index of connectivity in an upland landscape, where surface topographic controls on rainfall routing are dominant. They found that despite being a static, spatially-derived statistic it could explain a significant proportion of the variability in the probability and duration of a point connecting by surface flow to the drainage network. However, its impact upon the time-dependent modeling of river flows and its use in investigations of the effects of land management activities upon runoff generation has yet to be considered.

The second major challenge in the Topmodel framework is that the timing of delivery of water from sub-catchments will have an effect on the hydrograph. This timing is a function of the distribution of travel times resulting from the spatial position of each zone contributing runoff *within* each contributing area. This can be particularly important in relation to diffuse land management impacts as these may change, for instance, the speed with which overland flow can be delivered to the drainage network.

Here, we address this challenge by coupling the Network Index of Topmodel to a spatially-distributed unit hydrograph approach (e.g. Maidment, 1993; Maidment *et al.*¸1996; Olivera and Maidment, 1999; Saghafian *et al.*, 2002; Liu *et al.* 2003; Du *et al.*, 2009) that uses the time to equilibrium (t_e) approach pioneered by Saghafian and Julien (1995). We make three assumptions: (1) a single continuous and time-invariant flow path within a storm event (e.g. Maidment *et al.*, 1996) but allowing for the effects of modifications to these flow paths by land management activities; (2) a linear system response in which at higher flows, travel times are independent of the amount of runoff being routed (e.g. Kull and Feldman, 1998; Olivera and Maidment, 1999); and (3) independence of response where two locations share elements of the same flow path (e.g. Maidment *et al.*, 1996). Spatially-distributed unit hydrograph approaches have been found to reproduce the rapid runoff component of measured hydrographs extremely effectively (e.g. Maidment *et al.*, 1996). We recognize that travel time treatments should change with the amount of runoff being generated and delivered from upstream contributing areas (Saghafian *et al.*, 2002) but we view this as a future model development.

We modify the spatially distributed unit hydrograph to account for the spatial pattern of saturation in the catchment. The critical topographic index value above which a cell is saturated can be calculated from the catchment average storage deficit using equation 1. We generate a separate unit hydrograph for each topographic index class then combine them to generate the hydrograph for all overland flow producing areas. We define three flow domains (hillslope, grip, channel) each with an associated average velocity. We calculate the travel time through each domain for each cell by combining its flow path length through that domain with its velocity. We then sum these travel times to calculate the total travel time for that cell and generate a frequency distribution of travel times for all cells in that topographic index class. Overland flow produced by cells in the topographic index class is then routed to the outlet according to its travel time distribution.

It is worth emphasizing that in the default Topmodel version, with and without the Network Index treatment, there is still a routing treatment based upon delaying overland flow at each sub-catchment outlet by an estimate of the time for translation to the downstream catchment outlet. This is retained in our default treatments. By adopting a spatially-distributed unit hydrograph approach, our analysis allows for time of travel effects at the within sub-catchment scale which may be critical in situations where land management measures change significantly the timing associated with overland flow and hence subsurface flow paths (e.g. surface drains).

Methodology

Model application

In summary, The above model developments allow for four different model structures: (I) the default Topmodel; (II) Topmodel with a Network Index treatment alone, which only allows generated overland flow to leave the catchment if there is saturation along the flow path from the site of generation to the drainage network; (III) Topmodel with the proposed SDUH treatment alone, which controls the speed with which runoff reaches and travels through the drainage network according to the flow paths followed; and (IV) Topmodel combined with both the Network Index and proposed SDUH.

The Oughtershaw Beck sub-catchment

The model was applied to Oughtershaw Beck sub-catchment of the River Wharfe, North Yorkshire (Figure 1). The catchment area is 13.8 km^2 with an altitudinal range of 297 m from a low point of 353 m above Newlyn Datum. The catchment was artificially drained by grips during the 1970s, before which it was primarily blanket peat. We had access to 5 m resolution IfSAR elevation data collected during Intermap's NEXTmap Britain campaign and supplied through the U.K.'s Environment Agency. We use the terrain model (DTM) in which non-ground points, (e.g. trees, buildings and walls) have been removed since these can act as unrealistic barriers to both subsurface and overland flow. Milledge *et al.* (2009) have shown that these data are reliable for this kind of environment.

Two sets of hydrological data were available for the project, supplied by the U.K.'s Environment Agency, and associated with an initiative that started in 1997, the Upper Wharfedale Best Practice Project, designed to improve our understanding of how catchment management might be used to address hydrological and water quality problems in upland catchments: (1) a continuously recording rain gauge, which provided 15 minute interval precipitation data; and (2) a stage recorder at the catchment outlet, which has been coupled with spot flow gaugings to produce a stage-discharge relationship and hence a continuous record of discharge. Evidence suggested that when the flow reaches bankfull, at about 2.2 m^3s^{-1}, the form of the relationship is less well-established due to the difficulty of measuring these high flows directly. Thus, the peak flows, in particular, have some uncertainty associated with them.

Model application

The model was applied with an hourly time-step, chosen to reflect measured rates of change of discharge in the catchment. We generated the topographic index for the catchment using the 5 m resolution DTM and calculating: slope using the Zevenbergen and Thorne (1987) algorithm; and upslope contributing area using the multiple flow algorithm (Quinn *et al.*, 1991) after filling sinks using the Planchon and Darboux (2002) method. Table 1 summarises the model application in terms of the parameters associated with the model, their initial values, and their revised values in response to calibration. In the absence of climate data, we chose to treat the proportion of rainfall (effective rainfall, ER) available for infiltration into the soil column as an adjustable parameter. The following sections detail the calibration and model assessment steps in full. In summary, we began by undertaking a single parameter perturbation sensitivity analysis for each structural version of the model to identify sensitive parameters, with sensitivity quantified with reference to a set of Objective Functions defined below. Then, for sensitive parameters, we undertook a Monte Carlo (MC) type sensitivity analysis, sampling very wide parameter ranges, and used these results to produce a narrower set of plausible parameter ranges. These narrower ranges were intensively resampled using MC methods to identify a set of parameter ranges that defined the calibrated model. These ranges were then: applied in the same MC framework to a randomly chosen period of data not used in the calibration process to provide a split sample test; and also used to generate a set of model predictions including parameter uncertainty. Finally, the model was applied with and without grips, again in the same MC framework, to see if there were significant changes in hydrological response given parameter uncertainty.

Model sensitivity analysis

The analysis is based upon the assumption that the check data, the downstream flow gauge, provides a reliable time series of river discharge. Our first stage of analysis is to reduce the number of parameters influencing model behaviour so as to undertake a more intensive sampling of parameter space in a Monte Carlo framework. Thus, we set the expected parameter values in Table 1 based upon a combination of literature review and previous experience. We then undertake a doubling and a halving of each parameter, one at a time (see Campologno, 2000; Saltelli *et al.*, 2000) and quantify the response of a suite of objective functions to these parameter changes. We undertake the one at a time analysis for each structural combination of the model (i.e. I to IV above). Following McCuen (1973) quantification of the one at a time analyses is based upon Relative Sensitivity (RS) that compares the linear rate of change of each objective function to the rate of change of each parameter and standardizes these rates of change by the ratio of the mean of the parameter values used to the mean of the objective function values derived:

$$R_s = \left| \frac{dOF}{dP} . \frac{< P >}{< OF >} \right| \qquad [2]$$

Following Beven (2000), we do not use the one at a time analysis as a means of inferring model performance. Rather, we use it: (1) to assess whether model response to parameter perturbation is as expected (e.g. expected directions of change); and (2) to reduce the number of parameters that need to be included in the Monte Carlo based uncertainty analysis, which is computationally intensive, but which allows for a finer resolution exploration of model response. One particular issue arises with this analysis: where model response to parameter perturbation is non-linear the parameter range explored could be in a zone that is asymptotic or strongly parabolic. We moderated this issue by considering the extent to which those parameters identified as most sensitive fitted with prior expectations and through visually exploring how model output was responding.

Central to this stage of the work, and the uncertainty analysis described below, was selection of a suite of Objective Functions to quantify the relationship between model predictions and field observations. We focus upon undertaking model uncertainty analysis and model calibration with reference to the outlet discharge. Rather than using a single Objective Function, we considered a suite of Objective Functions (Table 2) and aimed to look for: (1) parameters that were generally sensitive across multiple Objective Functions; and (2) parameters that during the one at a time analysis suggested strong sensitivities but for perhaps only one or two of these Objective functions.

Model uncertainty analysis and calibration

In the second stage of the analysis, those parameters identified as being sensitive using one at a time analysis were subject to a Monte Carlo based uncertainty analysis. We chose this methodology because we expected that parameter interactions could condition model response significantly and we approached the analysis using a two-stage methodology. We used it as part of model calibration by using the Objective Function set, as obtained for model runs with wide parameter ranges, to narrow those parameter ranges in the next set of runs. Then, the analysis was repeated using this narrowed parameter ranges.

First, for those parameters identified as sensitive, we specified a parameter range based upon literature review and prior experience which encompassed the range of plausible parameter values (Table 1, Monte Carlo (MC) Run 1). We then randomly sampled 30,000 times within these parameter ranges making no *a priori* assumptions about the possible distribution of parameter values within those ranges. The same set of parameter ranges was applied to all four model structures to produce 120,000 model runs. For each model structure (i.e. I to IV), we ranked each parameter set for each Objective Function. We calculated the mean and standard deviation of parameter values associated for each ($n + k$) ranks for each Objective Function, for $n = 10$ and $k = 0 : 5000$. We then used significance testing to see the extent to which the mean and standard deviation for each of the $n : k$ parameter values differed from the *a priori* set of parameter values, for each Objective Function.

Second, we used the significance testing above to refine the parameter ranges to those shown in Table 1 (MC Run 2). The mean and standard deviation of parameters that resulted in the best Objective Functions varied as a function of both k and Objective Function, with the widest standard deviations in all cases found for the largest k. Thus, we defined the lowest value for each parameter range as the minimum of the set of (mean - standard deviation) values for all Objective Functions; and the highest values as the maximum of the set of (mean + standard deviation) values for all Objective Functions, with the mean and standard deviation calculated for the $n : k$ parameter values found to be significantly different from the *a priori* range. For the second run, as with the first, we sampled within these refined ranges making no prior assumption about the distribution of possible parameter values between ranges because: (1) although the parameter ranges are based upon distributions (i.e. mean and standard deviations), they are based upon a composite analysis of the ensemble set of all means and standard deviations; and (2) we did not believe that these prior means and standard deviations were based upon a sufficiently fine sample of the parameter space for them to be entirely reliable at this stage.

After MC Run 2, we were able to undertake a number of analyses. First, to understand model uncertainty, to assist with the identification of equifinality and to further constrain optimal model parameter values, we produced two-dimensional probability density functions (e.g. Figure 2) showing the percentage of data points found in each combination of parameter value and Objective Function for all Objective Functions. We did this for each model structure to understand the effects of different model structures on the associated uncertainty. Second, we considered the relative performance of all 120,000 MC Run 2 simulations to see if, given parameter uncertainty, it was possible to identify differences between different model structures. Third, for each model structure (i.e. I to IV) we also repeat the process of ranking each parameter set for each Objective Function and then plotting the mean and standard deviation of parameter values associated with each ($n + k$) ranks for each Objective Function, for $n = 10$ and $k = 0 : 5000$ (e.g. Figure 3). This allows us to identify and to compare the parameter values that optimize the Objective Functions for each model structure. It also allows us to identify how many simulations, for each model structure, have parameter values not significantly different (at $p = 0.05$) from the complete parameter set used in the second MC run. Where the number of simulations is high, the model is effectively strongly equifinal with respect to that parameter. Where it is low, that parameter tends to require a constrained range of possible parameter values. Fourth, we used the Objective Functions to weight the calculation of a mean predicted discharge and an associated standard deviation of predicted discharge. This weighting function was based upon the assumption that each Objective Function should be given equal weight in the weighting process. For each simulation, the linear distance between a given Objective Function for that simulation and the optimal value of that Objective Function for all simulations was determined. This was then scaled linearly by the range of values of that Objective Function simulated for all simulations. For each simulation, this produced one weight for each Objective Function. The six weights were multiplied together for each simulation and divided by the sum of the multiplied weights across all simulations. These weights were used in the calculation of the mean and standard deviation of model predictions. The weights are determined linearly because we have no other information to support a more complex calculation.

Finally, we sought to identify the structure and parameter values required for a calibrated model by looking at the intersection of optimized parameter ranges for each Objective Function. We identify the possible parameter range for a given Objective Function and parameter as the mean ± 1.96 standard deviations. We then cross-compare these parameter ranges using statistical significance testing and use this as the basis of a final, calibrated parameter range.

Split sample test

In order to provide some assessment of the calibrated model, and recognizing the lack of additional sites suitable for model testing, we applied the model to a randomly selected, non-overlapping, time period of the same duration, such that we could assess the model against data not used in the uncertainty and calibration exercise. We randomly sampled 1000 parameter sets from the calibrated parameter ranges and applied these parameter sets to this second time period of data, using the combined model. We calculated the mean and standard deviation of each Objective Function for the 1,000 simulations. We repeated this step for the calibration period. Finally, we compared the results for the randomly selected time period with the calibration period.

Assessment of open drain impacts upon hydrological response

We assess the effects of removing grips upon hydrological response under the assumption that there is no change in the parameter ranges required for the model to be calibrated. We discuss this issue after the results have been presented.

Model development: results and discussion

One at a time sensitivity analysis

Table 3 shows the results from the one at a time sensitivity analysis and confirms substantial variability in the Relative Sensitivity of model parameters. For the default formulation, the effective rainfall (ER) has the highest relative sensitivity across almost all objective functions, followed by the Topmodel parameter m and transmissivity (T_o). Introduction of the network index correction does not change this substantially, except that some objective functions become slightly more sensitive to variation in m and, slightly fewer, more sensitive to T_o. These results are in marked contrast to the introduction of the spatially-distributed unit hydrograph treatment. Comparison with the default model suggests substantially greater sensitivity of most objective functions to variations in m and T_o and reduced sensitivity of some objective functions to variations in ER. Thus, the model structure used impacts upon the ways that parameters interact sufficiently to be detected in Objective Functions. As the spatially distributed unit hydrograph increases both the number of parameters available and the sensitivity of objective functions to default model parameters it both offers a wider range of calibration options but also raises the greater possibility of equifinality for different parameter combinations. For the purpose of exploring this equifinality, the analysis also identifies a number of parameters that can be discounted on the basis of exceptionally low levels of relative sensitivity. We set the threshold for inclusion as any parameter with a relative sensitivity for one or more objective functions $>10^{-5}$. These are flagged in bold in Table 3, and include six parameters for the default and Network Index versions and the same six parameters plus three SDUH parameters in situations when the spatially-distributed unit hydrograph treatment is used.

Uncertainty analysis

Table 1 shows the parameter ranges used in the first MC run and then the refined values applied to the second MC run. Results from applying the refined parameter values during the second MC run are shown as probability density functions (pdfs) for each Objective Function and each Parameter in Figure 2 for the combined model (i.e. including both the Network Index and SDUH modifications). Figure 2 shows that a small number of parameters have a substantial impact upon most Objective Functions. Other parameters show equifinality when judged against some or all Objective Functions in that a wide range of parameter values produces equally plausible outcomes. Three parameters appear to be particularly important. First, the hillslope velocity results in consistently worse Objective Functions for values less than 0.1 ms^{-1} and, but to a less notable extent, for values greater than 0.2 ms^{-1} (Figure 2). Second, the pdfs for the two Topmodel soil parameters, m and T_o, also appear to have preferential Objective Function values although, as with the hillslope velocity, there is also substantial scatter. The soil parameters constrain the sensitivity of runoff generation to rainfall: higher values of m cause a more rapid reduction in hydraulic conductivity with depth, so making saturated conditions easier to generate; lower values of T_o, reduce the effective rate of lateral throughflow through the soil column, so having the same effect. Thus, taken together, the Objective Functions for the combined model are most sensitive to parameters that control the rate of rapid runoff generation (i.e. propensity to saturation) and its transport over hillslopes to the channel, whether a drain or a stream. Parameters introduced to control the speed of routing through the grips and streams show clear equifinality with good and poor Objective Functions obtained for all values of the parameters used and this provides a first indicator that the effects of grips upon the hydrograph through the speed of delivery effect may not be particularly significant.

Figure 3 shows the mean ± standard deviation of the set of k simulations with Objective Functions better than the k^{th} simulation, again for the combined model. The x plotting point is the Objective Function for the k^{th} simulation and in all cases the Objective Functions are sorted so that Objective Functions degrade from left to right. Figure 3 allows slightly more conclusive observations to be made. In interpreting Figure 3, if a mean parameter value changes as a function of Objective Function, then this suggests that there is some association between the parameter values being used and the Objective Functions that result. If the standard deviation is close to this mean and then widens as the Objective Function degrades, it suggests that the best model simulations require a relatively narrow range of values of that parameter. Eventually, once all simulations are considered (i.e. k = 30,000), the curves will approach the mean ± standard deviation of the original parameter range used in the second MC run. This allows the possibility of significance testing to identify the proportion of simulations that, for each parameter and each Objective Function, is not significantly different from the mean of the parameter range used. A high proportion of simulations suggests that a wide range of parameter values will optimize the model and the model is, in effect, equifinal with respect to that parameter/Objective Function combination.

Figure 3 suggests that five of the nine parameters used in the Combined Model have a particular influence on model performance: IRZS; m; T_o; ER; and hillslope velocity. For hillslope velocity and T_o, and to a lesser extent m, and across most, if not all, Objective Functions, the standard deviation of parameters that deliver a given level of performance increases rapidly. This suggests that these parameters need to be tightly constrained in order to deliver the best model solutions. The levels of equifinality in the Combined Model (Table 4) reflect the importance of these five parameters: they are associated with generally lower levels of equifinality than the other four parameters. However, there is some variation in the importance of these five parameters between Objective Functions. For example, for *m*, RMT has relatively high level of equifinality, suggesting that *m* is not an important control on the timing of flood peaks. This in marked contrast to hillslope velocity which has higher levels of equifinality for Objective Functions based on global model performance (i.e. MUE, NSE) but much lower levels of equifinality for Objective Functions that assess prediction of individual or a small number of flow peaks (i.e. PQE, RMQ, RMT). The peak discharge error needs particular comment. Although the peak discharge error has variable levels of equifinality when different parameters are compared (Table 4), Figure 3 shows that standard deviations of the parameter values that optimize the Objective Function are generally wide across all parameter ranges. Either the model does not capture the peak discharge correctly or the peak discharge is in error. Whereas the other flood peaks recorded in the record were only slightly larger than the bankfull flow, and so close to the calibration range of the stage-discharge relationship at Oughtershaw, the largest peak (from which the peak discharge error was calculated) was substantially higher than the range maximum, and therefore potentially in error, especially as we do not allow ER to rise (and hence modeled flows to fall) within a storm event.

Figure 4 shows mean and standard deviation of the weighted mean model predictions of discharge, with the associated standard deviation, for the Combined Model as compared with the observed flow. The observed flow is generally bracketed by the ±95% standard deviation and shows that for the significant majority of time the model has been calibrated effectively on the measured discharge given parameter uncertainty. Table 5 shows the ranges of parameter values recommended in subsequent use of the model for this catchment and rainfall record and which we used for the split testing of the model.

Split sample test

Figure 5 shows the results of the split sample test for the six Objective Functions used for the uncertainty analysis. None of the distributions of Objective Functions are significantly different (at p=0.05) from those obtained during the calibration period suggesting that the calibrated parameter ranges do hold for this second period.

Model structure and uncertainty analysis

Thus far, the uncertainty analysis has focused upon the properties of the Combined Model. Here, we compare this Combined Model with the Default Model and the Network Index only and SDUH only treatments. Figure 6 shows the result of ranking all simulations for all model structures (i.e. 120,000 simulations) and then comparing where in this rank order different structural versions of the model appear. We do this for all Objective Functions. To illustrate the interpretation of Figure 6, with a global excedance probability of 0.4 in Figure 6a, the model structure excedance probability is 0.6 for the Combined Model: around 60% of the Combined Model simulations appear in the best 40% of all model simulations. The striking pattern in Figure 6 is that the curves for the SDUH model versions, whether with or without the Network Index, plot clearly above the Default and Network Index only versions, except for the RMQ Objective Function. The extent to which this is the case varies between Objective Functions. It is clearest in relation to the RMT where over 80% of both models involving the SUH correction appear in the best 50% of all simulations. The SDUH model versions also dominate the best 10 to 20% of all simulations for MUE and NSE. Thus, it appears that the SDUH delivers better model predictions notwithstanding parameter uncertainty.

The Network Index versions of the model are less clear. On its own, it performs more effectively for MUE, NSE and COR but it's simulations appear generally lower in the rank order than the SDUH only model. Adding in the Network Index version to the SDUH treatment does not appear to result in a clear improvement relative to the SDUH only model, as whilst the PQE and COR are marginally better, the MUE, NSE and RMQ are very marginally worse. Thus, the conclusion is that the Network Index correction does not seem to have a significant impact upon hydrograph representation in this case.

Figure 7 shows the ranked mean and standard deviation of parameter values, plotted against Objective Function, for just two of the parameters (m and T_o) obtained using the Default Model. Comparing Figure 7a and 7b with Figures 3b and 3c respectively shows statistically significant ($p>0.05$) changes in the parameter values for *m* and T_o and IRZS that optimize model performance. The standard deviations associated with parameter values that produced the very best Objective Function values are also narrower. This is confirmed in Table 4, which shows that levels of equifinality in the Default Model are generally much lower, especially for T_o, implying that in the Default Model these parameter values matter much more. Figure 7 shows that the Default Model requires lower values of *m* and higher values of T_o.

Discussion

The above results suggest that central to representing the measured discharge record in the study catchment using Topmodel is a Spatially-Distributed Unit Hydrograph treatment. The SDUH modification produced the best model simulations across all six Objective Functions considered, even given parameter uncertainty (Figure 6), although it introduced three new parameters (velocities for the hillslope, grips and channels). Of these three, the hillslope velocity was found to be of particular importance, requiring values between 0.1 and 0.2 ms^{-1} when judged across all Objective Functions in order to obtain optimal model performance (Figure 2). This range is interesting in comparison with some of the very few data obtained on overland flow velocities for upland peat catchments (Holden *et al.*, 2008). Holden *et al.* showed that the overland flow velocities depended on vegetation cover, slope and flow depth, a much more complex set of controls than we include here, but had typical values only marginally smaller than those found to be optimal here.

Two of the Topmodel soil parameters, *m* and T_o, were also found to have preferential Objective Function values (Figure 3). Compared with the default model (Figure 7), higher *m* values and lower T_o values were required to optimize model predictions. Higher *m* implies a more rapid decline in hydraulic conductivity and lower T_o a slower lateral subsurface flux, making hillslope velocities more important. Thus, in the default model, the lack of representation of hillslope velocity at the within hydrological response unit scale is delivered by increasing the lateral subsurface flux to greater levels (lower *m*, harder to generate overland flow; higher T_o, greater lateral subsurface flux). This is the sense in which *m* and T_o represent effective parameters in the default model, producing the right effect albeit for the wrong reasons. The problem with effective parameterization in the default case is that changing *m* and T_o will impact upon other elements of process representation, such as the propensity to generate overland flow, which will be reduced as well as the initial soil moisture conditions at the start of the storm event. Further, as Table 4 shows, introducing the SDUH treatment, although this results in new data needs, it increases the level of equifinality associated with two parameters, themselves with an exceptionally poor resemblance to possible field process measurements. Equifinality can arise for two fundamentally different reasons: (1) for model realisations that matter which cannot be resolved by the data available; and (2) where a parameter generally is of less importance than others. Whilst (1) might be a negative interpretation of the identification of equifinality in a model (*cf.* Hamilton, 2007), (2) is an important finding if the objective is the production of a minimally-complex, perhaps parsimonious, model.

The difficulty of effective parameterisation is confirmed in Figure 8, which shows the behaviour weighted model predictions and observed discharge for each model structure, illustrating a critical effect of the SDUH correction: it introduces some hydrograph smoothing in a way that produces more realistic hydrographs when compared with the observed discharge. Whilst effective parameter values may be used to optimise Objective Functions (cf. *m*, Figure 7a) there may be a limit to which they can capture critical hydrological processes. In this catchment, it appears that the spatial distribution of flow routing that the SDUH captures is critical, and its lack of inclusion is only partially compensated for through parameterization. It is important to be critical of the assumption that a more complex model, which introduces more parameters, is problematic because it increases the difficulty of identifying unique parameter sets. Here, strong interactions between parameters, as well as those interactions introduced with the more complex model, did not increase levels of equifinality. Rather, adding parameters changed the hydrological response of other elements of the system in ways that made them more meaningful. Most importantly, the split testing of model predictions showed no significant changes in model performance when the same parameter ranges were used in the model for a second, non-overlapping time-period.

Assessment of drain impacts

Figure 9 shows the effects of the global removal of grips as compared with the gripped case. We emphasise that this will not be the same as blocking all of the grips in the catchment because field evidence suggests that blocking grips does not immediately and necessarily result in the restoration of intact peat (Holden *et al.*, 2011), although there may be some parallels. It is clear from Figure 9 that the dominant effect of grip removal in this catchment is to produce higher peak flows and lower base flows, suggesting that it is the rearrangement of the drainage and increase in catchment wetness following grip removal which dominates over the reduction in overland flow velocity. Superimposed on this are some apparent reductions in peak flow when grips are removed, but these are entirely produced by changes in timing (of one or two time steps) of the flood peak. Thus, the results confirm the observation that blocking grips leads to raised water tables (e.g. Price *et al.*, 2003; Holden, 2005; Worrall *et al.*, 2007; Armstrong *et al.*, 2010; Wilson *et al.*, 2010) and a greater tendency to surface saturation and so overland flow (e.g. Shantz and Price, 2006) during storm events. Figure 10 shows the change in topographic index associated with grips, showing the spatially extensive potential for reductions in surface saturation associated with gripping. Figure 10 is calculated without representing any changes in soil or vegetation characteristics that follow from gripping, indicating that there will be a substantial impact upon catchment wetness associated with the rearrangement of surface drainage patterns (effectively changes in upslope contributing area) even before other effects are considered. The more effective removal of water increases soil moisture deficits, so making it more difficult to generate floods in a gripped landscape.

What is perhaps surprising is that this is not countered in any way by the theoretical changes arising from surface overland flow being routed into drains, especially given the differences in optimal grip and hillslope velocities (Table 5). There are a number of potential reasons for this, which we evaluate here. First, it is possible that introducing grips increases velocities for some flow paths, but increased flow path lengths counter this, especially as grips were commonly installed along contours, preventing water from following the downslope route. The extent to which this is the case will depend on the grip network and how it is laid out in the catchment. Our analysis shows that introducing grips increases flow path lengths by more than one cell width in 2.1% of cases, but generally reduces flow path lengths (41.0% of cases), suggesting that this is an unlikely hypothesis. Indeed, Figure 11a shows that the gripped case has a very similar frequency distribution of flow path lengths to the intact case. However, Figure 11b and 11c demonstrate a more important and second possibility. They show the frequency distributions of the time required for delivery to the catchment outlet from the onset of a rainstorm for all grid cells. In theory, the more kurtotic this distribution, the greater the proportion of the catchment area that delivers flow at the same time. Figure 11b shows that with the default hillslope velocity of 0.15 ms^{-1} and grip velocity of 0.45 ms^{-1}, introducing grips does not appear to increase the kurtosis significantly but, rather, shifts the entire distribution marginally towards shorter times. Increasing the grip velocity to 0.90 ms^{-1} does not change this observation significantly. Thus, for the catchment outlet considered here, the grips do not change the peak flow, but they do cause that peak to occur marginally earlier. Figure 12 shows the cumulative distributions of the data in Figure 11b. For the majority of the distribution, the curves are parallel, but shifted, suggesting the shape of the distribution does not change, but the position of the distribution does. Figure 13 quantifies these results for a range of grip and hillslope velocities. First, it shows that for all hillslope velocities, introducing grips does marginally reduce the mean time required for delivery to the catchment outlet (Figure 13a) but this is countered by small reductions in the level of kurtosis, or peakiness (Figure 13b). These reductions are small, but they show that despite grips having potentially greater local velocities, it is the interactions of these effects, as would be controlled by grip density and location at the level of the drainage network, that determines how grip velocities change the kurtosis of the delivery times. In this case, they are reduced. Second, and reflecting the results of the uncertainty analyses reported above (Figures 2, 3), the dominant control on the sensitivity of the catchment scale hydrological response is the hillslope flow velocities (Figure 13). The reason for this dominance is illustrated in Figure 14, which shows that the majority of each flow path is hillslope and that drainage only changes this marginally (between 5 and 10%), restricting the effects that grips can have upon the travel times to the catchment outlet.

The above discussion leads to three critical observations. The first is a network effect, in which the structure of the drainage basin controls the degree and the timing of runoff concentration in the network (travel time concentration), and hence flood peaks. In this example, the density and layout of grips, in relation to the structure of the drainage network, is such that the reduction in travel times due to increased grip velocities do not translate into greater travel time concentration. The second is a relative effect. Although grips marginally reduced the level of travel time concentration (Figure 13b) compared to the intact case for the catchment outlet considered here, they also marginally reduced the mean travel times. Thus, the catchment as a unit responds marginally earlier. Whether or not this has an impact downstream will depend both on general flow attenuation but also how this altered timing relates to other downstream contributing catchments. The impacts of grips are entirely relative and scale dependent. Third, and most importantly, because hillslopes maintain the highest proportion of flow path lengths, even with gripping, it is the hillslopes that dominate the hydrological response. In this study, we have not considered possible roughness changes associated with between-drain, hillslope zones. The transition to drier surface conditions could both increase this roughness (where there is a transition to more shrubby vegetation, such as *Ericacea* spp); but it could also reduce it, especially with degradation of organic matter in the surface layer and possible erosion to leave a bare soil surface, with velocity characteristics more similar to those of the drains themselves (albeit with depth-related velocity differences).

There are some important caveats to the results that are reported here. First, the emphasis here has been upon comparison of the intact and gripped case. Extending the results to grip blocking needs caution. It is possible that a more strategic removal of grips might still be beneficial, especially where their removal is designed to reduce the concentration of travel time distributions. Second, the SDUH treatment that we have used is as simple as it can be: we take no account of variations within the catchment in travel times related to slope, changes in overland flow depth during a storm event, and the roughness values associated with differences in land cover. Given the experiments in Figures 12 and 13, the magnitude of the differences that would need to be associated with these effects for the grip velocity effect to have an impact would have to be much greater than the differences between these variables that have been measured in the field (see Holden *et al.*, 2008). Our findings probably hold notwithstanding the relative simplicity of the SDUH treatment we use. Third, draining the peat will have caused changes to the soil system such as the development of soil pipes (e.g. Holden, 2006). Removing grips may not reverse this process initially and it may be some time before there is a return to an intact peat system (Holden et al., 2011). Thus, there are likely to be leads and lags in the actual hydrological response to grip removal that will remain in the system and which are not represented in the model that we include here. Fourth, the model does not explicitly represent infiltration-excess overland flow. In a heavily degraded peatland system, it is possible that bare peat becomes relatively hydrophobic with very low infiltration rates, and increased probability of infiltration-excess overland flow. It may be that the storage effect of peat is much reduced such that removing grips does not lead to changes in catchment wetness, as what is dominant is the already-reduced infiltration rates associated with peat degradation. Finally, further research is required, probably by comparison with more physically-based representations (e.g. Ballard *et al.* 2009, 2011), to assess the extent to which the physical basis of the model presented here is sufficient. However, such research is unlikely to undermine the critical observation reported herein: the reduction in attenuation often thought to be associated with faster drain velocities linked to upland drains may be substantially countered by the ways in which the drains change the shape of the drainage network, ultimately increasing flow path lengths.

Conclusions

This paper describes a model for assessing the impacts of shallow upland drains, grips, upon flow hydrographs in a form that allows for calibration and uncertainty analysis; and applies this model to explore the effects of global removal of grips. The model development showed that representing the hydrological response of the study system required the classic Topmodel to be combined with a spatially-distributed unit hydrograph treatment. Correction for the effects of disconnected saturated zones, following Lane *et al.* (2004) was found to be less important. Strong interactions were found between parameters and the analysis of model performance showed that: (1) parameters in the classic Topmodel compensated partially for the effects of not including a spatially-distributed unit hydrograph treatment; and (2) that introducing this treatment, although providing more parameters, reduced rather than increased levels of model equifinality. More complex models, with more parameters, may not increase model equifinality if the sensitivity of model predictions to those parameters is relatively high.

Grip removal produced significantly higher flood peaks and lower baseflows, even given parameter uncertainty, reflecting the characteristics commonly reported from field observations. This was primarily related to the effect of grips on creating drier antecedent conditions, as compared with the effects of grips upon reducing travel times to the catchment outlet and so reducing attenuation. In fact, in the catchment studied here, faster flow velocities in the grips did not contribute to an increase in flood peaks because: grips comprise a small proportion of most total flow path lengths, and the structure of the drainage network also mitigates the grip velocity effect. Significantly, it is necessary to assess whether a particular grip network increases or reduces the concentration of travel times, as indicated by a statistic such as kurtosis. In addition, a small number of grips actually increased flow path lengths, countering velocity effects. Far more important appears to be the extent that grips change the surface vegetation and thus hillslope flow velocities.

These changes need to be considered at the catchment scale for two reasons. First, the spatial structure of the grip network in the catchment has to be considered. Second, a distinction has to be made between: (a) changes in travel time concentration arising from grips, as compared with the intact case, which may or may not increase local flow magnitudes in the catchment; and (b) changes in the timing of catchment response, which may increase or decrease downstream flows, according to how other tributary catchments are responding. Even if grip velocity effects dominate over soil moisture effects, the impact of upstream drainage on downstream flood magnitude depends entirely on where you measure it in the catchment.

Acknowledgements

This work was supported by a grant from the Environment Agency of England and Wales and was undertaken in collaboration with the Yorkshire Peat Project and the Yorkshire Dales Rivers Trust. Joe Holden and a second reviewer provided very valuable reviews of the first draft of this manuscript.

References

Ahti, E., 1980. Ditch spacing experiments in estimating the effects of peatland drainage on summer runoff. International Association of Hydrological Sciences Special Publication, **130**, IAHS, Wallingford, 49–53.

Armstrong, A. **, 2010. The impact of peatland drain-blocking on dissolved organic carbon loss and discolouration of water; results from a national survey. *Journal of Hydrology*, 381, 112–120.

Baden, W. and Eggelsmann, R., 1970. Hydrological budget of high bogs in the Atlantic region. Proceedings of the 3rd International Peat Congress, 1968, Quebec. Department of Energy, Mines and Resources, Ottawa, 260–311.

Ballard, C.E., Wheater, H.S., McIntyre, N., and Bulygina, N., 2009. Modelling the effects of land use change on peatland hydrology. Paper presented at a British Hydrological Society Meeting, July 2009. Downloaded 27.06.11 from http://workspace.imperial.ac.uk/civilengineering/public/3_BHSpeat2009.pdf

Ballard, C.E., Wheater, H.S., McIntyre, N., Holden, J. and Wallage, Z., 2011. The development of a physically-based model of drained peatlands. Poster presented at the British Hydrological Society Upland Hydrology Meeting, Leeds. Downloaded 27.06.11 from http://workspace.imperial.ac.uk/civilengineering/public/1_Peat%20Poster2.pdf.

Ballard, C.E., McIntyre, N., Wheather, H.S., Holden, J. and Wallage, Z., in press. Hydrological modeling of a drained blanket peatland. Forthcoming in *Journal of Hydrology* **

Beven, K., and Freer, J., 2001. Equifinality, data assimilation, and uncertainty estimation in mechanistic modelling of complex environmental systems using the GLUE methodology. *Journal of Hydrology*, 249, 11–29

Beven, K.J. and Kirkby, M.J., 1979. A physically-based, variable contributing area model of basin hydrology. *Hydrological Sciences Bulletin*, 24, 43-69.

Beven, K.J. and Wood, E.F., 1983. Catchment geomorphology and the dynamics of runoff contributing areas. *Journal of Hydrology*, 65, 139-158.

Beven, K.J., 1997. TOPMODEL: A critique. In Beven, K.J. Distributed Hydrological Modelling: Applications of the TOPMODEL concept, Wiley, Chichester, 1-17.

Burke, W., 1967. Principles of drainage with special reference to peat. *Irish Forestry* 24, 1–7.

Burt, T.P., Labadz, J.C. and Butcher, D.P. 1997. The hydrology and fluvial geomorphology of blanket peat: implications for integrated catchment management. In Tallis, J.H., Meade, R. and Hulme, P.D., (eds), *Blanket Mire Degradation*, British Ecological Society, 121–27.

Campolongo, F., Kleijnen, J. and Andres, T., 2000. Screening Methods. In Saltelli, A., Chan, K. and Scott, M. (eds.) *Sensitivity Analysis*, Wiley, New York, 65-80.

Conway, V.M. and Millar, A., 1960. The hydrology of some small peat-covered catchments in the northern Pennines. *Journal of the Institute of Water Engineers*, 14, 415–24.

Du, J.K., Xie, H., Hu, Y.J., Xu, Y.P. and Xu, C.Y., 2009. Development and testing of a new storm runoff routing approach based on time variant spatially distributed travel time method. *Journal of Hydrology*, 369, 44-54.

Evans, M., Burt, T.P., Holden, J. and Adamson, J.K. 1999. Runoff generation and water table fluctuations in blanket peat: evidence from UK data spanning the dry summer of 1995. *Journal of Hydrology,* 221, 141–60.

Guertin, D.P., Barten, P.K. and Brooks, K.N., 1987. The peatland hydrologic impact model: development and testing. *Nordic Hydrology*, 18, 79–100.

Gunn, J. and Walker, C., 2000. Peat cutting and bog restoration. In Gunn, J. (ed.) *The geomor- phology of Culcagh Mountain, Ireland: a field guide for the British Geomorphological Research Group spring field meeting*. Limestone Research Group, University of Huddersfield, 15–25.

Hamilton S. 2007. Just say NO to equifinality. Hydrological Processes, 21, 1979–1980.

Holden, J., 2005. Peatland hydrology and carbon cycling: why small scale process matters. *Philosophical Transactions of the Royal Society*, A363, 2891– 2913.

Holden, J., 2006. Sediment and particulate carbon removal by pipe erosion increase over time in blanket peatlands as a conse- quence of land drainage. *Journal of Geophysical Research* 111, F02010.

Holden, J., Burt, T.P., Evans, M.G. and Horton, M., 2006. Impact of land drainage on peatland hydrology. *Journal of Environmental Quality*, 35, 1764–1778.

Holden, J., Chapman, P.J. and Labadz, J.C., 2004. Artificial drainage of peatlands: hydrological and hydrochemical process and wetland restoration. *Progress in Physical Geography*, 28, 95-123.

Holden, J., Chapman, P.J., Lane, S.N and Brookes, C.J., 2006. Impacts of artificial drainage of peatlands on runoff production and water quality. In Martini, I.P., Cortizas, A.M. and Chesworth, W. (editors) Peatlands: basin evolution and depository of records of global environmental and climatic changes, Amsterdam, Elsevier, 501-28.

Holden, J., Kirkby, M.J., Lane, S.N., Milledge, D.G., Brookes, C.J., Holden, V. and McDonald, A.T., 2008. Overland flow velocity and roughness properties in peatlands. *Water Resources Research*, 44, W06415.

Howe, G.M. and Rodda, J.C., 1960. An investigation of the hydrological cycle in the catchment area of the river Ystwyth during 1958. *Water and Water Engineering*, 767, 10–16.

Kull, D.W. and Feldman, A.D., 1998. Evolution of Clark's unit graph method to spatially distributed runoff. *ASCE Journal of Hydraulic Engineering*, **, 9–19.

Lane, S.N., Brookes, C.J., Holden, J. and Kirkby, M.J., 2004. A network index based version of TOPMODEL for use with high resolution digital topographic data. *Hydrological Processes*, 18, 191-201.

Lane, S.N., Reaney, S.M. and Heathwaite, A.L., 2009. Representation of landscape hydrological connectivity using a topographically driven surface flow index. Water Resources Research, 45, W08423, doi:10.1029/2008WR007336.

Lewis, W.K. 1957. An investigation or rainfall, runoff and yield in the Alwen and Brenig catchments. *Proceedings of the Institution of Civil Engineers*, 8, 17–52.

Liu, Y.B., Gebremeskel, S., De Smedt, F. Hoffman, L. and Pfister, L., 2003. A diffusive transport approach for flow routing in GIS-based flood modelling. *Journal of Hydrology*, 283, 91-106.

Maidment, D.R., 1993. Developing a spatially distributed unit hydrograph by using GIS. In Kpvar, K. and Nachtnebel, H. (eds) Applications of Geographical Information Systems in Hydrology and Water Resource Management, International Association of Hydrological Sciences Special Publication 211, 181-92.

Maidment, D.R., Olivera, F., Calver, A., Eatherall, A. and Fraczek, W., 1996. Unit hydrograph derived from a spatially distributed velocity field. *Hydrological Processes*, 10, 831-44.

McCuen, R.H., 1973. The role of sensitivity analysis in hydrologic modeling. *Journal of Hydrology*, 18, 37-53.

McDonald, A.T., 1973. Some views on the effects of peat drainage. *Scottish Forestry* 27, 315–27.

Milledge, D.G., Lane, S.N. and Warburton, J., 2009. Digital filtering of generic topographic data in geomorphological research. *Earth Surface Processes and Landforms*, 34, 63-74

Newson, M.D. and Robinson, M. 1983. Effects of agricultural drainage on upland streamflow: case studies in mid-Wales. *Journal of Environmental Management*, 17, 333–48.

Oliver, J., 1958. The wetness of Wales. Rainfall as a factor in the geography of Wales. *Geography* 43, 151–63.

Olivera, F. and Maidment, D.R., 1999. Geographic information systems (GIS)-based spatially distributed model for runoff routing. *Water Resources Research*, 35, 1155-64.

Planchon O., and Darboux F. 2002. A fast, simple and versatile algorithm to fill the depressions of digital elevation models. *Catena*, 46, 159-176.

Price, J.S., Heathwaite, A.L. and Baird, A.J. 2003. Hydrological processes in abandoned and restored peatlands: an overview of management approaches. *Wetlands Ecology and Management*, 11, 65–83.

Quinn, P., Beven, K., Chevallier, P. and Planchon, O., 1991, The prediction of hillslope flow paths for distributed hydrological modeling using digital terrain models. *Hydrological Processes*, 5, 59-80.

Ramchunder, S.J., Brown, L.E. and Holden, J., 2009. Environmental effects of drainage, drain-blocking and prescribed vegetation burning in UK upland peatlands. *Progress in Physical Geography*, 33, 49-79.

Robinson, M., 1980. The effect of pre-afforestation drainage on the streamflow and water quality of a small upland upland catchment. Institute of Hydrology Report, 73, IAHS, Wallingford.

Robinson, M., 1985. The hydrological effects of moorland gripping: a re-appraisal of the Moor House research. *Journal of Environmental Management*, 21, 205–11.

Robinson, M., 1986. Changes in catchment runoff following drainage and afforestation. *Journal of Hydrology*, 86, 71–84.

Robinson, M. and Armstrong, A.C., 1988. The extent of agricultural field drainage in England and Wales, 1971–1980. *Transactions of the Institute of British Geographers*, 13, 19–28.

Saghafian, B. and Julien, P.Y., 1995. Time to equilibrium for spatially variable watersheds. *Journal of Hydrology*, 172, 231-45.

Saghafian, B., Julien, P.Y. and Rajaie, H., 2002. Runoff hydrograph simulation based on time variable isochrone technique. *Journal of Hydrology*, 261, 193-203.

Saltelli, A., Chan, K. and Scott, M. (eds.), 2000. *Sensitivity Analysis*, Wiley, New York.

Saulnier, G-M., Obled, C. and Beven, K.J., 1997. Analytical compensation between DTM grid resolution and effective values of saturated hydraulic conductivity within the TOPMODEL framework. In Beven, K.J. Distributed Hydrological Modelling: Applications of the TOPMODEL concept, Wiley, Chichester, 249-64.

Shantz, M.A. and Price, J.S. 2006. Characterization of surface storage and runoff patterns following peatland restoration, Quebec, Canada. *Hydrological Processes*, 20, 3799–814.

Stewart, A.J.A. and Lance, A.N., 1983. Moor-draining: a review of impacts on land use. *Journal of Environmental Management*, 17, 81–99.

Stewart, A.J.A. and Lance, A.N., 1991. Effects of moor-draining on the hydrology and vegetation of northern Pennine blanket bog. *Journal of Applied Ecology* 28, 1105–17.

Wilson, L., Wilson, J., Holden, J., Johnstone, I., Armstrong, A. and Morris, M., 2010. Recovery of water tables in Welsh blanket bog after drain blocking: Discharge rates, time scales and the influence of local conditions. *Journal of Hydrology*, 391, 377-86.

Worrall, F., Armstrong, A., and Holden, J., 2007. Short-term impact of peat drain- blocking on water colour, dissolved organic carbon concentration, and water table depth. *Journal of Hydrology*, 337, 115–125.

Zevenbergen, L.W. and Thorne, C.R., 1987. Quantitative analysis of land surface topography. *Earth Surface Processes and Landforms*, 12, 47-56.

Tables

Table 1. Model parameters, mid-point values used in one at a time sensitivity analysis, sensitivity identified from this analysis, parameter ranges used for the Monte Carlo simulations and final recommended parameter ranges.

Parameter	Mid-point values used in one at a time sensitivity analysis	One at a time sensitivity	MC Run 1 Parameter Range	MC Run 2 Parameter Range	Rec. min.	Rec. mid.	Rec. max.
IRZS Initial depth of water stored in the root zone (m)	0.002	Yes	0.001 : 0.100	0.002 : 0.050	0.010	0.015	0.020
Maximum depth og water that can be stored in the root zone (m)	0.02	No				0.02	
M Topmodel *m* parameter, which controls the rate od decline of transmissivity with increasing storage deficit	0.01	Yes	0.001 : 0.100	0.002 : 0.050	0.040	0.045	0.050
T_o Transmissivity (m^2s^{-1})	1	Yes	0.10 : 10.00	0.20 : 1.00	0.37	0.40	0.43
UZTD Unsaturated zone time delay (hours)	50	Yes	1.0 : 100.0	30.0 : 70.0	40.0	48.0	56.0
InitQS Initial subsurface flow (m/hr)	0.0000328	Yes	0.00001 : 0.00010	0.00005 : 0.00090	0.00065	0.00075	0.00085
ER Effective rainfall (proportion of rainfall entering the nonsaturated zone)	0.50	Yes	0.20 : 1.00	0.60 : 0.80	0.65	0.67	0.69
CV Channel Velocity (ms^{-1})	1	Yes	0.001 : 1.000	0.30 : 0.80	0.46	0.56	0.66
HV Hillslope Velocity (ms^{-1})	0.01	Yes	0.001 : 1.000	0.01 : 0.60	0.10	0.15	0.20
GV Grip Velocity (ms^{-1})	1	Yes	0.001 : 1.000	0.20 : 0.80	0.35	0.45	0.55

Table 2. Objective Functions used in the analysis

Objective Function	Abbreviation	Units	Comments
Global Mean Unsigned Error	MUE	m^3s^{-1}	A measure of the average error. Main problem is that it places emphasis on all observations, when the focus is flow extremes. Retained as obtaining a generally robust hydrological representation we deemed to be important.
Error in the predicted magnitude of the largest measured discharge	PQE	m^3s^{-1}	An important measure given the focus of the modeling upon flood flows, but highly sensitive to errors in application of the stage-discharge relationship at high flows.
Nash-Sutcliffe Efficiency	NSE	None	The model efficiency, with behavioural models being defined as those with NSE values greater than zero. Maximum possible NSE value is 1. Main problem is that it places equal emphasis on all observations, when the focus is flow extremes. Retained as obtaining a generally robust hydrological representation we deemed to be important.
Root Mean Square Error in magnitude of predictions of the 10 largest observed discharges	RMQ	m^3s^{-1}	Recognises the importance of flood flows, but reduces the reliance upon the most extreme flood (and associated data uncertainty).
Root Mean Square Error in timing of predictions of the 10 largest observed discharges	RMT	m^3s^{-1}	Recognises the importance of flood flow timings as well as magnitudes.
Correlation	COR	None	A measure of the general association between variability in measured and predicted flows, that allows for representation of both magnitude and timing errors in a single statistic.

Table 3. Rs values for one at a time parameter perturbation results

Default Topmodel	MUE	Peak Q error	NSE	RMSE 10 largest Q	RMSE t, 10 largest Q	Correlation
IRZS	**0.00609**	0.00000	**0.01999**	**0.00212**	**0.00000**	**0.00113**
MaxRZS	0.00000	0.00000	0.00000	0.00000	0.00000	0.00000
m	**0.04894**	**0.97146**	**0.23321**	**0.01468**	**0.12118**	**0.04951**
To	**0.07152**	**0.17121**	**0.07060**	**0.26714**	**0.14270**	**0.01855**
UZTD	**0.00608**	**0.03354**	**0.04455**	**0.01793**	**0.00579**	**0.00631**
InitQS	**0.01931**	0.00000	**0.06163**	**0.01297**	**0.01905**	**0.00705**
ER	**0.10514**	**2.83000**	**2.59444**	**0.61590**	**0.01953**	**0.04147**
Network Index Version	MUE	Peak Q error	NSE	RMSE 10 largest Q	RMSE t, 10 largest Q	Correlation
IRZS	**0.00558**	0.00000	**0.01984**	**0.00212**	0.00000	**0.00114**
MaxRZS	0.00000	0.00000	0.00000	0.00000	0.00000	0.00000
m	**0.08683**	**1.77916**	**0.37903**	**0.00883**	**0.06701**	**0.04358**
To	**0.01321**	**0.23307**	**0.10922**	**0.21520**	**0.05612**	**0.00489**
UZTD	**0.00478**	**0.00651**	**0.03657**	**0.00819**	**0.01090**	**0.00232**
InitQS	**0.01794**	**0.00001**	**0.06504**	**0.01076**	**0.03658**	**0.00626**
ER	**0.15549**	**2.88014**	**2.43327**	**0.49573**	**0.10424**	**0.05769**
SDUH Version	MUE	Peak Q error	NSE	RMSE 10 largest Q	RMSE t, 10 largest Q	Correlation
IRZS	**0.00391**	0.00000	**0.05614**	**0.00179**	0.00000	**0.00548**
MaxRZS	0.00000	0.00000	0.00000	0.00000	0.00000	0.00000
m	**0.09465**	**0.24863**	**2.23016**	**0.12985**	**0.39662**	**0.11442**
To	**0.15546**	**0.90139**	**2.87724**	**0.11734**	**0.24857**	**0.06950**
UZTD	**0.00365**	**0.01052**	**0.11067**	**0.00215**	**0.13173**	**0.00409**
InitQS	**0.01313**	0.00000	**0.18708**	**0.00592**	**0.03299**	**0.01799**
ER	**0.02700**	**0.94978**	**0.15142**	**0.43482**	**0.27169**	**0.05175**
ChV	**0.00008**	**0.00101**	**0.00174**	0.00000	0.00000	**0.00039**
HV	**0.02388**	**0.22193**	**0.75358**	**0.02497**	**0.18678**	**0.00356**
GV	**0.00006**	**0.00062**	**0.00103**	**0.00003**	**0.00000**	**0.00014**
Combined Version	MUE	Peak Q error	NSE	RMSE 10 largest Q	RMSE t, 10 largest Q	Correlation
IRZS	**0.00458**	0.00000	**0.03185**	**0.00223**	**0.02639**	**0.00388**
MaxRZS	0.00000	0.00000	0.00000	0.00000	0.00000	0.00000
m	**0.14974**	**0.72361**	**1.49702**	**0.19080**	**0.40599**	**0.09535**
To	**0.13966**	**1.67111**	**1.39056**	**0.10415**	**0.08120**	**0.02979**
UZTD	**0.00434**	**0.01551**	**0.06673**	**0.00384**	**0.09225**	**0.00218**
InitQS	**0.01480**	**0.00001**	**0.10284**	**0.00702**	**0.03299**	**0.01243**
ER	**0.05015**	**1.29705**	**2.69030**	**0.55289**	**0.24001**	**0.04751**
ChV	**0.00008**	**0.00118**	**0.00077**	**0.00001**	**0.03299**	**0.00016**
HV	**0.04046**	**0.20354**	**0.34966**	**0.01232**	**0.06837**	**0.00404**
GV	**0.00008**	**0.00063**	**0.00029**	**0.00001**	**0.03299**	**0.00007**

Table 4. Levels of model equifinality (parameter definitions in Table 1): for each model structure, the percentage of parameter values that are not significantly different (at $p = 0.05$) from the complete parameter set used in the second MC run.

PARAMETER	IRZS	m	To	UZTD	InitQS	ER	ChV	HV	GV
1. Default									
MUE	49.6	33.2	4.1	100.0	100.0	6.0			
PQE	100.0	6.1	5.3	98.1	100.0	4.6			
NSE	69.6	16.7	4.2	97.9	100.0	4.9			
RMQ	78.5	13.5	4.7	100.0	100.0	4.9			
RMT	5.0	12.7	4.9	100.0	100.0	58.5			
COR	5.1	29.9	5.2	100.0	100.0	76.0			
2. Network Index									
MUE	39.9	44.8	4.0	92.4	100.0	10.5			
PQE	100.0	5.0	12.4	100.0	100.0	5.7			
NSE	59.1	17.4	4.9	90.1	99.3	5.4			
RMQ	64.0	14.7	7.1	100.0	99.9	6.0			
RMT	5.2	7.9	14.3	100.0	100.0	36.9			
COR	5.1	22.0	4.6	100.0	100.0	52.4			
3. SDUH									
MUE	30.0	21.7	6.9	100.0	100.0	10.6	81.4	5.9	100.0
PQE	99.3	5.1	8.0	99.8	99.8	4.8	100.0	7.3	100.0
NSE	48.5	11.4	4.9	100.0	100.0	5.2	81.6	5.9	100.0
RMQ	40.8	10.0	6.3	99.5	99.7	5.3	100.0	16.1	100.0
RMT	14.9	66.2	18.0	100.0	95.5	39.2	84.3	8.1	100.0
COR	5.2	27.1	13.6	100.0	100.0	59.7	100.0	6.9	100.0
4. Combined									
MUE	27.0	23.2	10.6	100.0	99.4	12.9	87.0	37.5	100.0
PQE	100.0	4.6	14.0	100.0	100.0	7.1	98.5	7.8	100.0
NSE	34.3	9.8	8.3	100.0	99.1	5.9	84.1	56.4	99.8
RMQ	38.0	8.4	12.5	100.0	99.8	6.2	100.0	12.7	95.4
RMT	14.4	77.4	17.8	100.0	88.7	39.9	100.0	6.5	99.3
COR	5.4	17.6	12.6	100.0	100.0	23.2	99.5	7.5	95.6

Table 5. Summary of final model calibration results, with 95% confidence limits

Mean Unsigned Error (m/s)	0.292 ±0.018
Mean Peak Discharge Error (cumecs)	-1.900 ±0.502
Mean Nash Sutcliffe Efficiency	0.700 ±0.042
Mean Root Mean Square Error in discharge for 10 largest flow peaks (cumecs)	1.020 ±0.164
Mean Root Mean Square Error in timing for 10 largest flow peaks (hours)	1.913 ±1.301
Correlation	0.869 ±0.055

Figures

Figure 1. map of the Oughtershaw study catchment showing the channel and drain (grip) networks and the stage gauge used in the analysis. The background map is elevation data (colours) and shaded relief from the 5 m resolution IfSAR DTM used in the model.

Figure 2. Probability density function plots derived for after the second Monte Carlo run using the combined model for the six objective functions (Figures 2a to 2i)

Figure 3. The mean and standard deviation of parameter values for all model realisations equal to or better than a given value of the Objective Function, for each Objective Function (3a to 3f), for the combined model. Plots are labelled such that best simulations are always closest to the y-axis.

Figure 4. Observed and predicted flows for the calibration period, showing 95% uncertainty limits.

Figure 5. Mean and standard deviation of Objective Functions obtained using the calibrated parameter ranges shown in Table 2 but applied to a second, randomly-selected and non-overlapping time period.

Figure 6. Rank performance of each model structure for each Objective Function

Figure 7. As per Figure 3, but using the default version of Topmodel, and showing results for the m and To model parameters only, for illustration.

Figure 8. Predicted and observed hydrographs for each model structure

Figure 9. Predicted discharges with and without grips.

Figure 10. Estimated change in topographic index as an index of soil moisture changes (blue shows where removing grips produces wetting; red, drying))

Figure 11. The distributions of total flow path length (11a) and the time required for delivery to the catchment outlet for grip velocities of 0.45 m/s (11b) and 0.90 m/s (11c), for the intact and gripped cases.

Figure 12. Cumulative frequency distributions of the time required for delivery to the catchment outlet for the intact and gripped cases.

Figure 13. The mean time required for delivery to the catchment outlet (13a) and the kurtosis in the distribution (13b) for different combinations of grip velocity and hillslope velocity. 0 refers to the case without grips. Kurtosis is non-dimensional, x 10^5.

Figure 14. Frequency distribution of the proportion of flow paths that are hillslope, for both the intact and the gripped case.

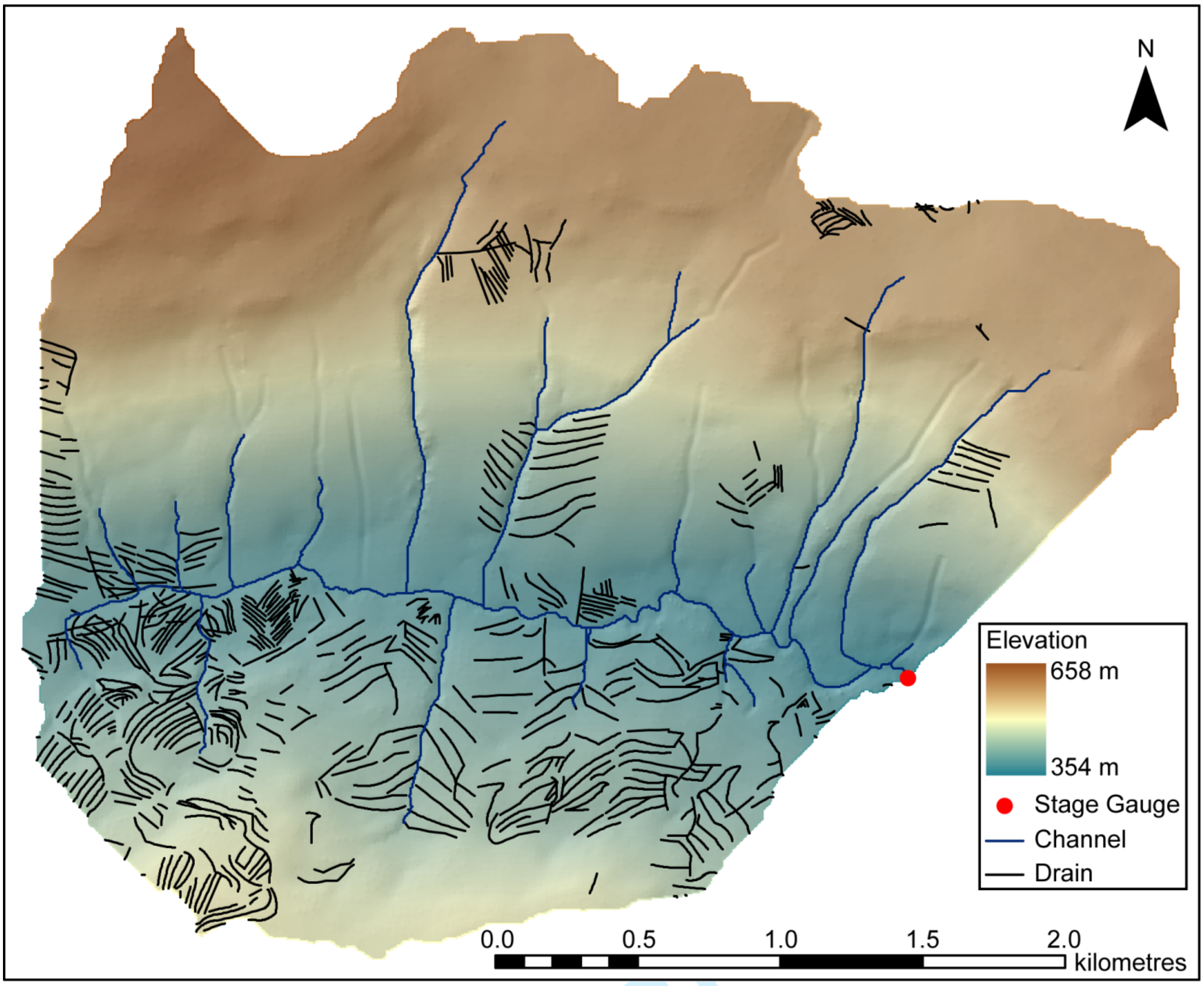
N
Elevation
658 m
354 m
Stage Gauge
Channel
Drain
0.0
0.5
1.0
1.5
2.0
kilometres

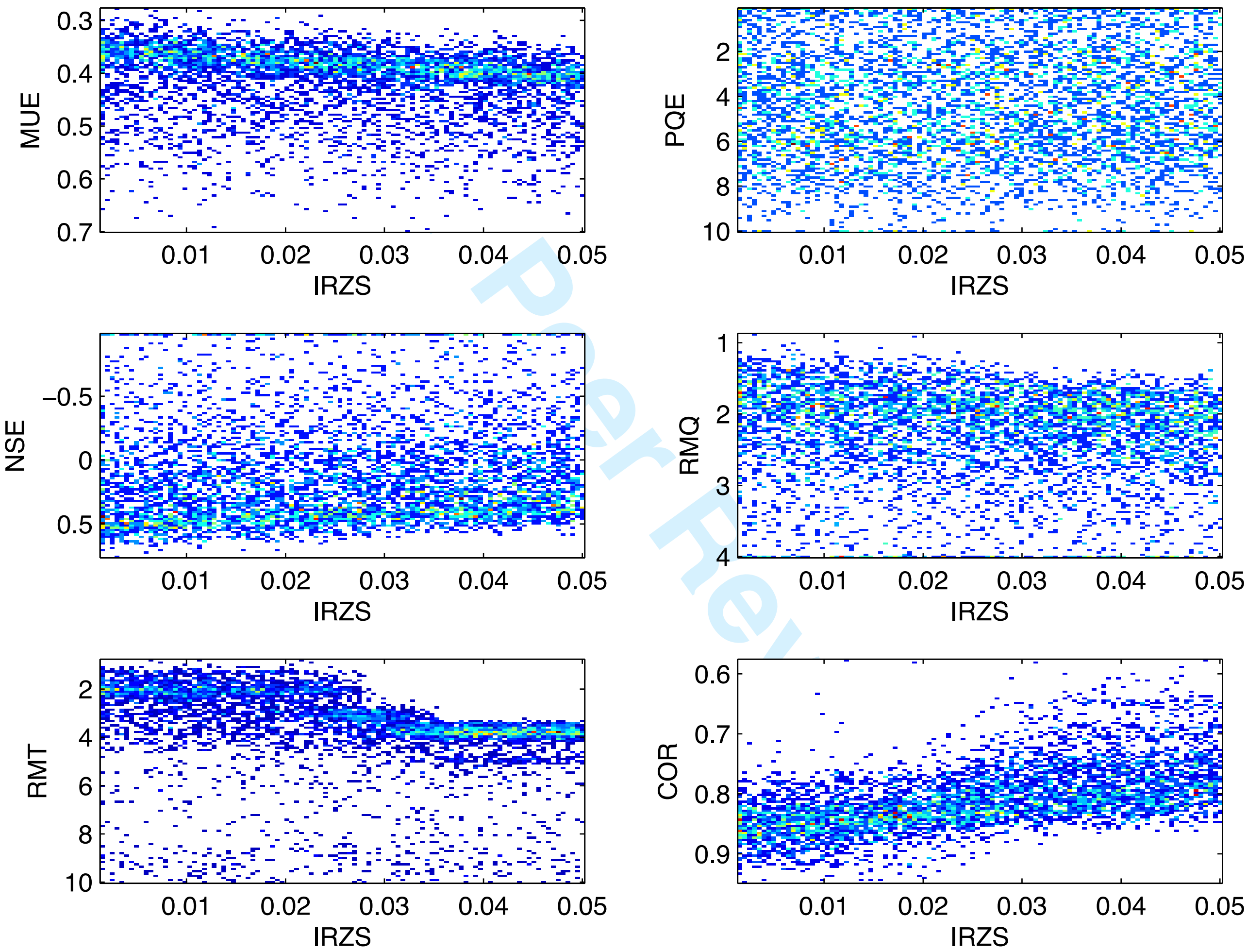
MUE
0.3
0.4
0.5
0.6
0.7
0.01
0.02
0.03
0.04
0.05
IRZS
PQE
2
4
6
8
10
0.01
0.02
0.03
0.04
0.05
IRZS
NSE
−0.5
0
0.5
0.01
0.02
0.03
0.04
0.05
IRZS
RMQ
1
2
3
4
0.01
0.02
0.03
0.04
0.05
IRZS
RMT
2
4
6
8
10
0.01
0.02
0.03
0.04
0.05
IRZS
COR
0.6
0.7
0.8
0.9
0.01
0.02
0.03
0.04
0.05
IRZS

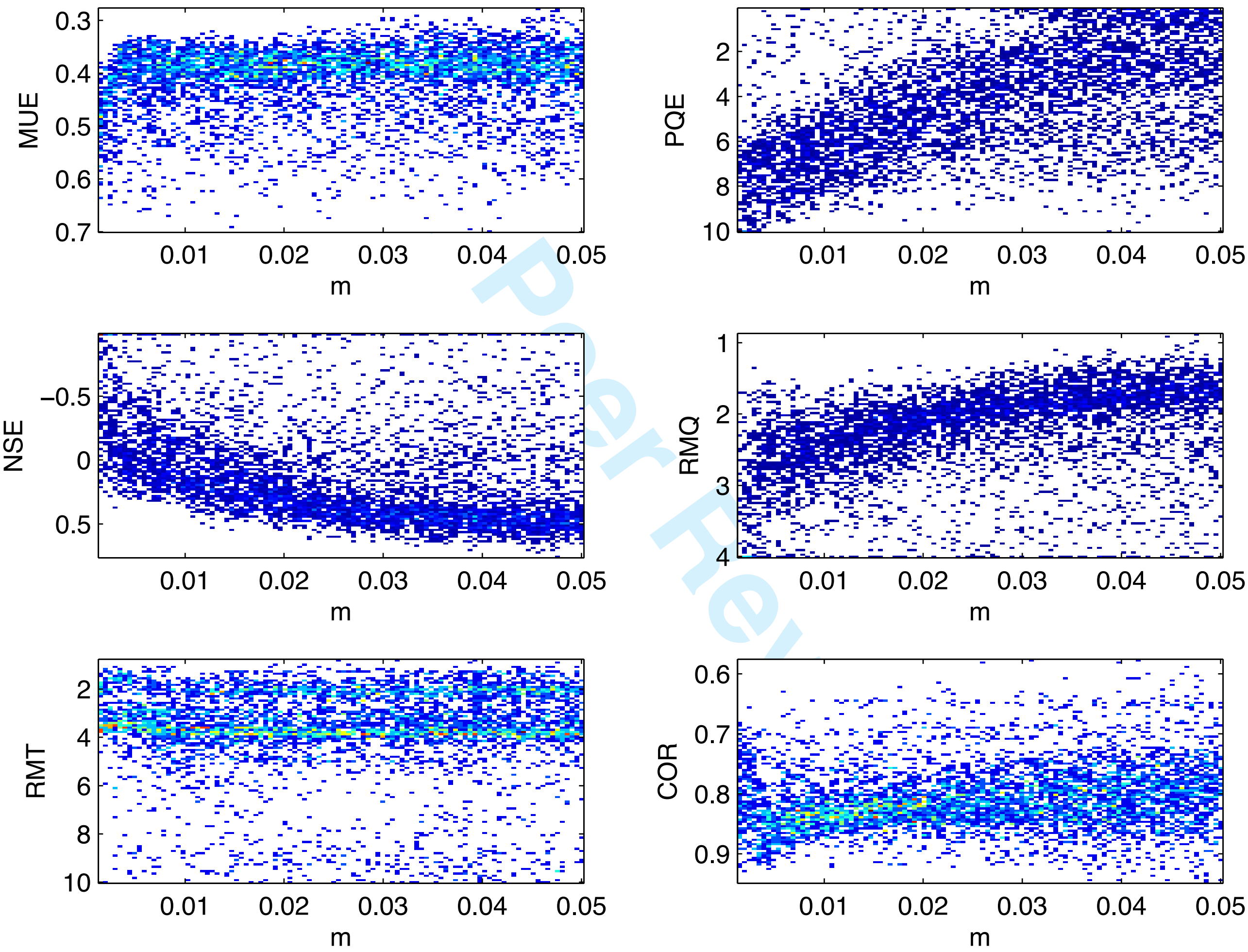
MUE
PQE
NSE
RMQ
RMT
COR
m
0.01
0.02
0.03
0.04
0.05

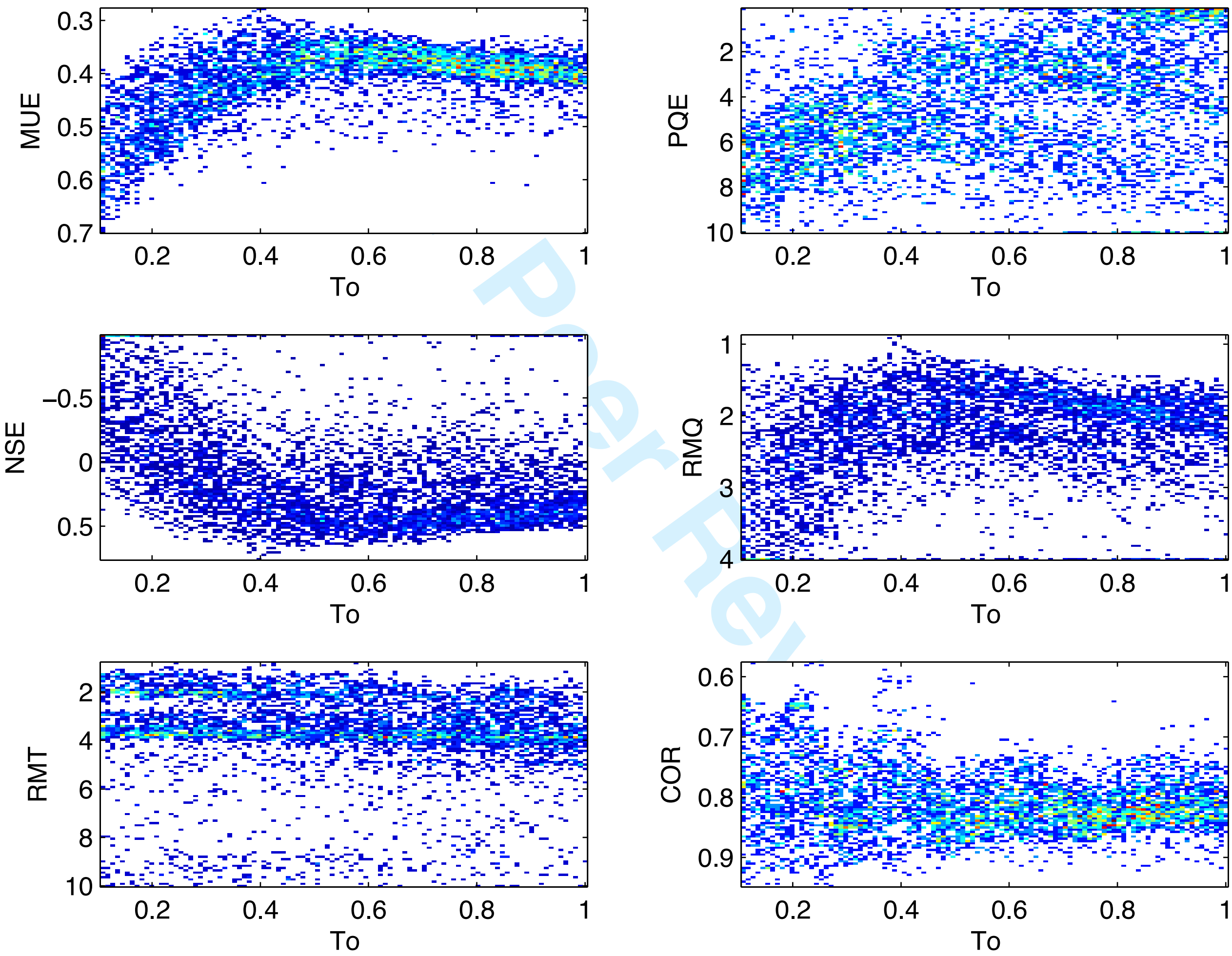
MUE
0.3
0.4
0.5
0.6
0.7
PQE
2
4
6
8
10
NSE
−0.5
0
0.5
RMQ
1
2
3
4
RMT
2
4
6
8
10
COR
0.6
0.7
0.8
0.9
0.2
0.4
0.6
0.8
1
To

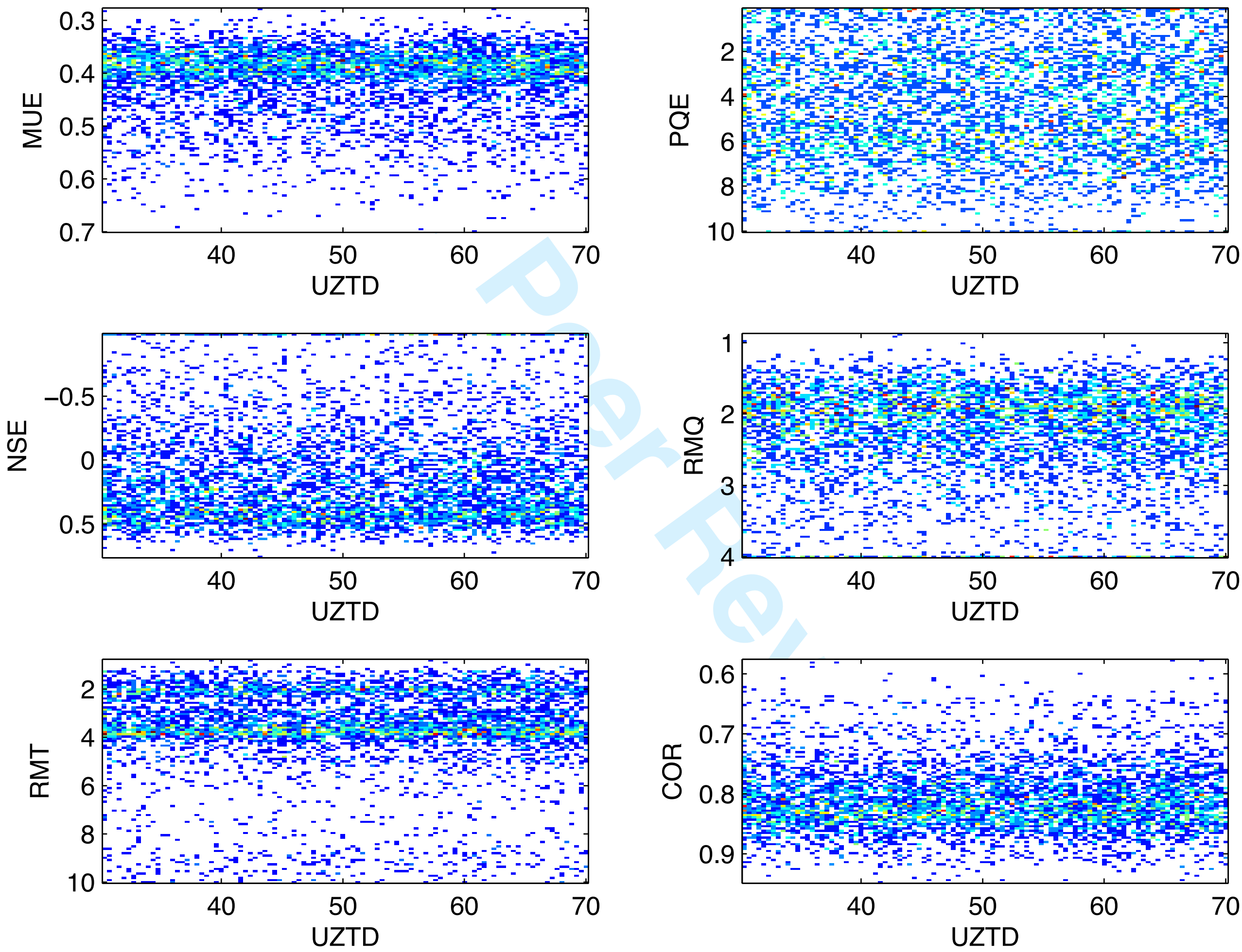
MUE
0.3
0.4
0.5
0.6
0.7
PQE
2
4
6
8
10
NSE
−0.5
0
0.5
RMQ
1
2
3
4
RMT
2
4
6
8
10
COR
0.6
0.7
0.8
0.9
40
50
60
70
UZTD

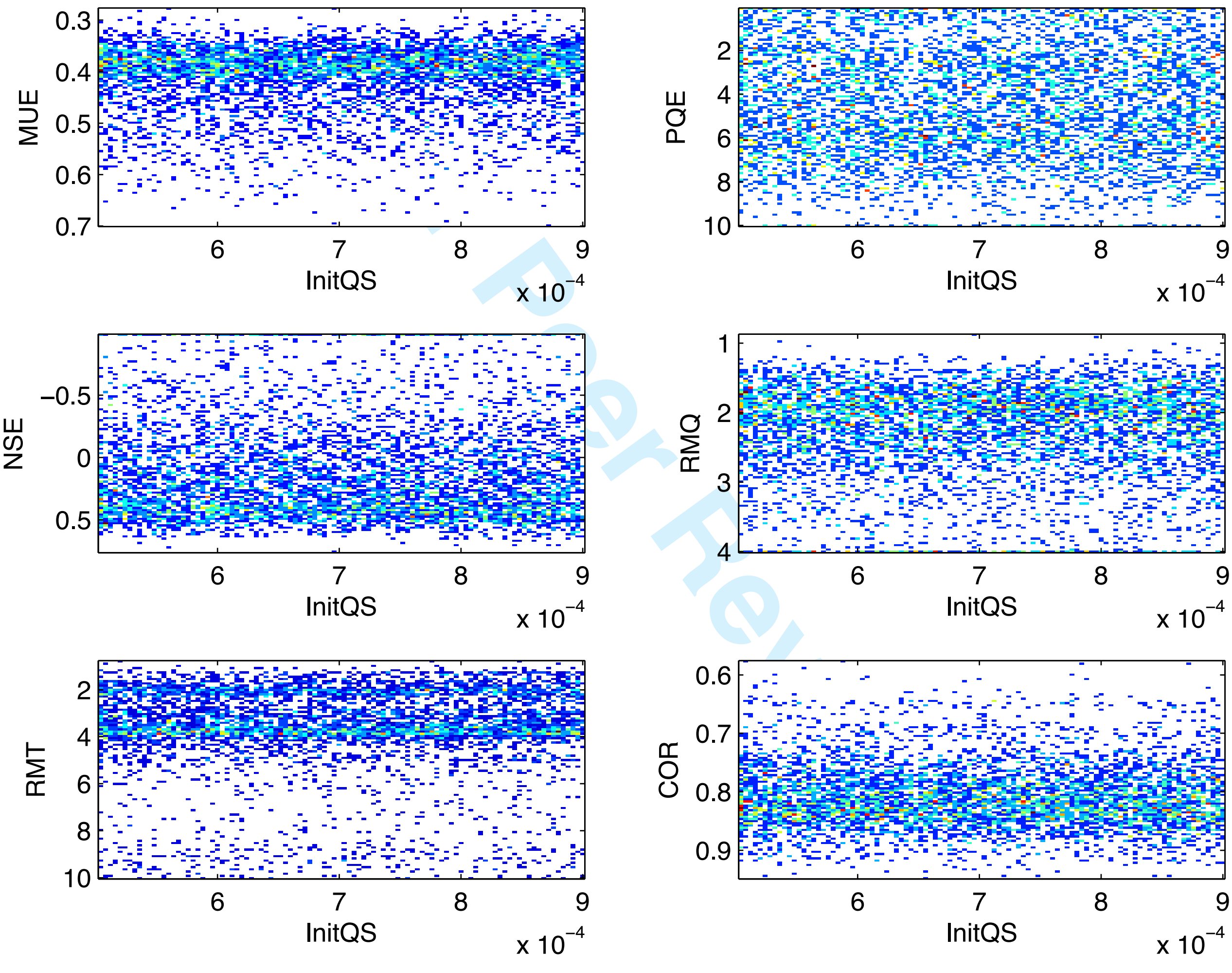

MUE
PQE
NSE
RMQ
RMT
COR
InitQS
x 10^-4

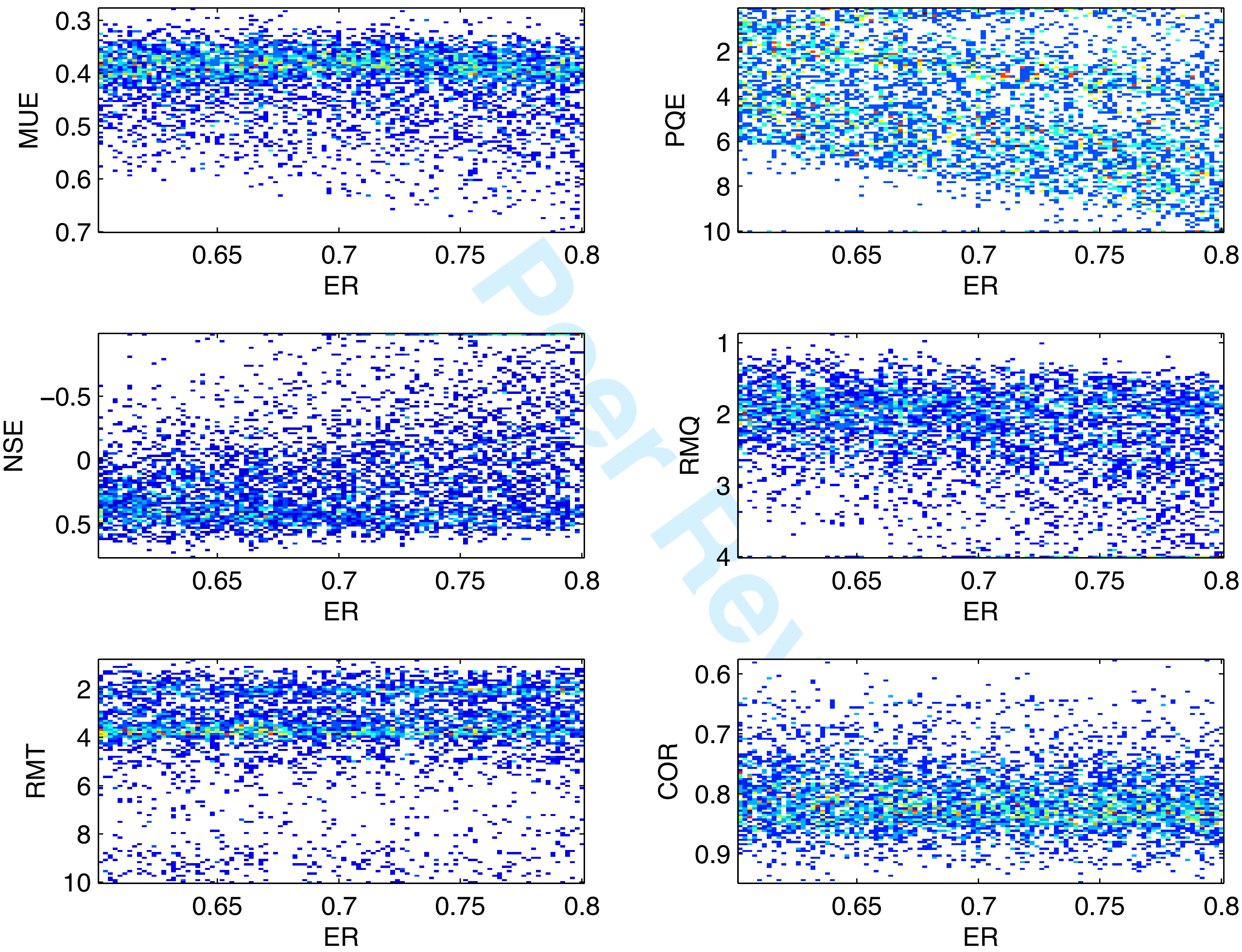
MUE
0.3
0.4
0.5
0.6
0.7
PQE
2
4
6
8
10
NSE
−0.5
0
0.5
RMQ
1
2
3
4
RMT
2
4
6
8
10
COR
0.6
0.7
0.8
0.9
0.65
0.7
0.75
0.8
ER

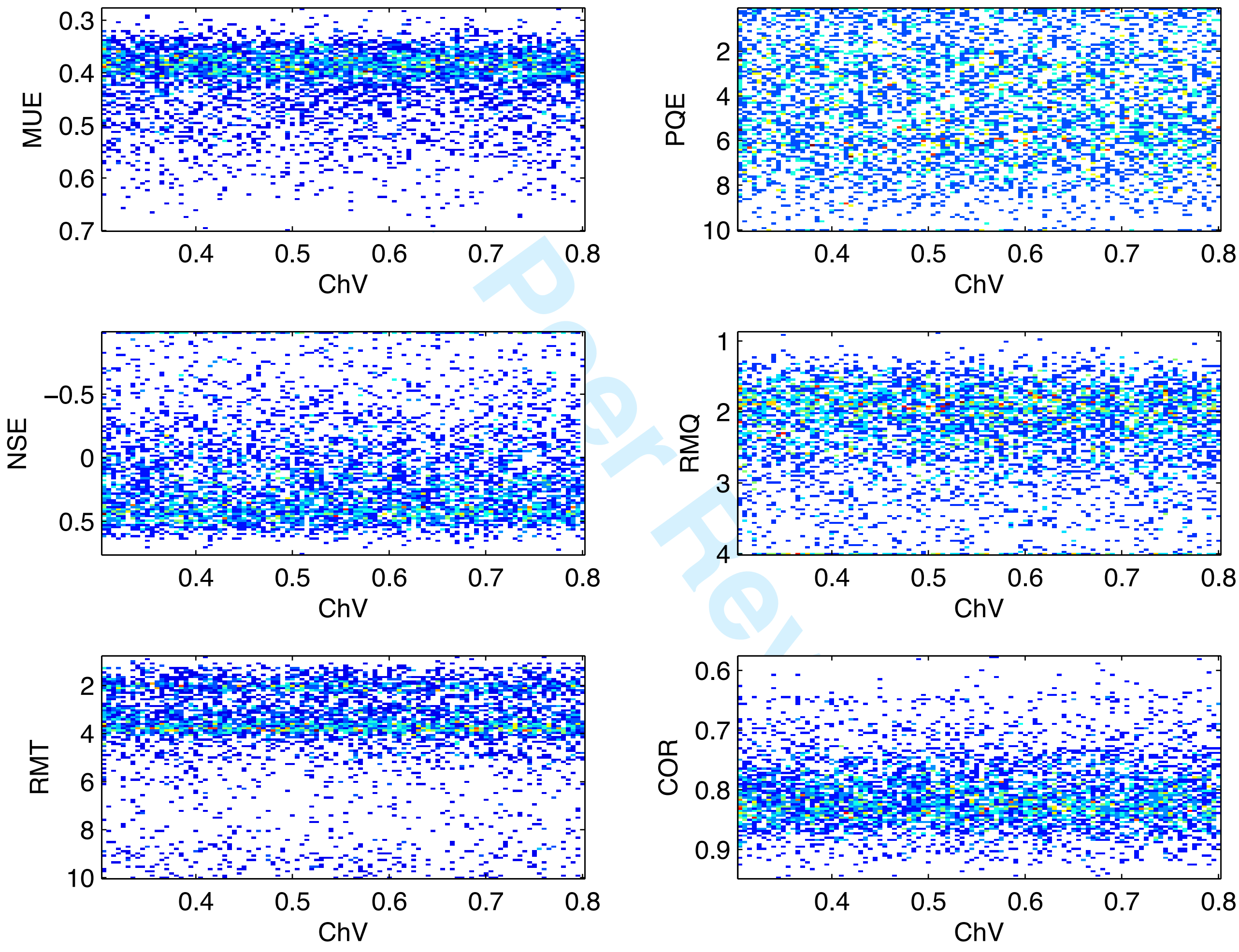
MUE
ChV
PQE
ChV
NSE
ChV
RMQ
ChV
RMT
ChV
COR
ChV

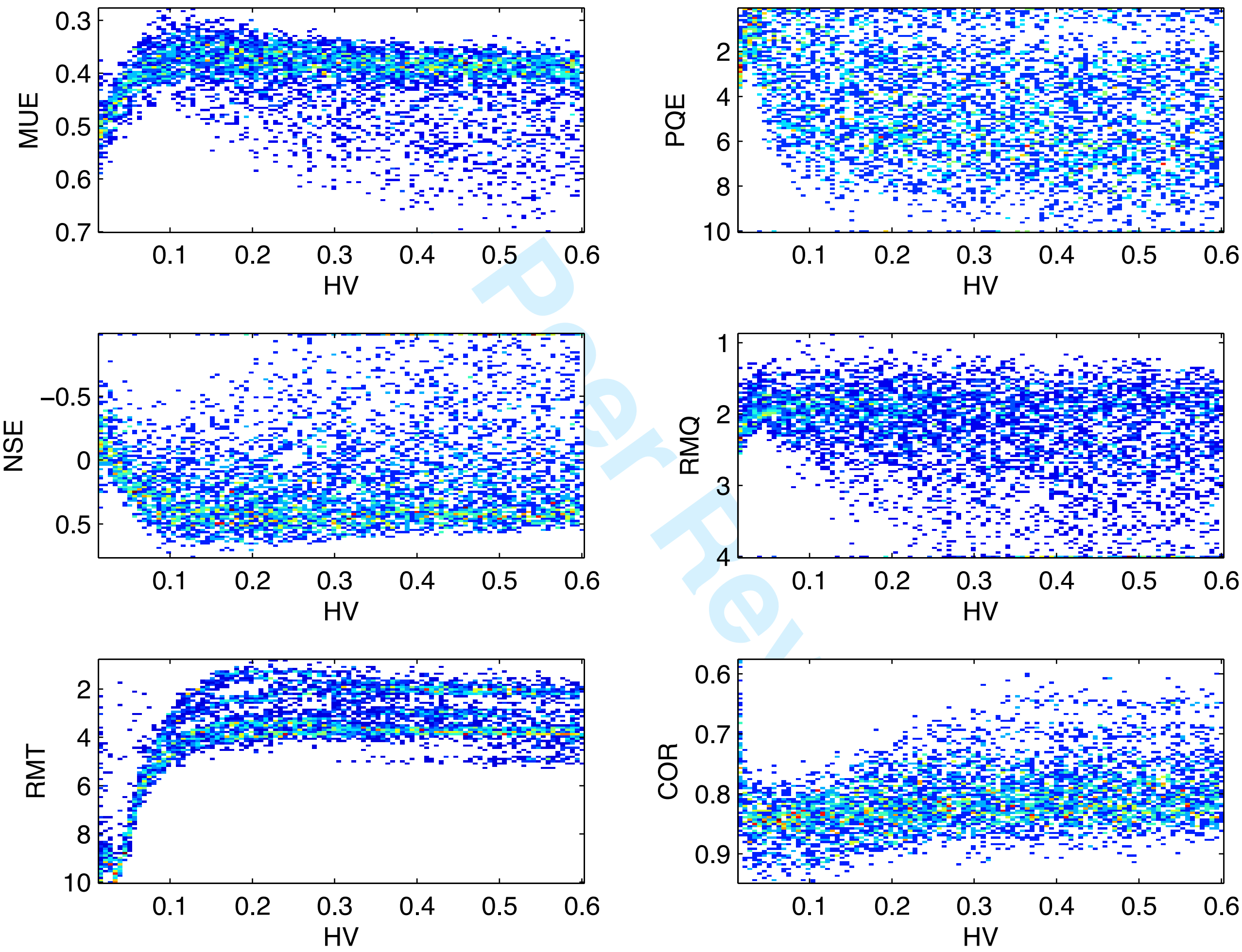
MUE
HV
PQE
HV
NSE
HV
RMQ
HV
RMT
HV
COR
HV

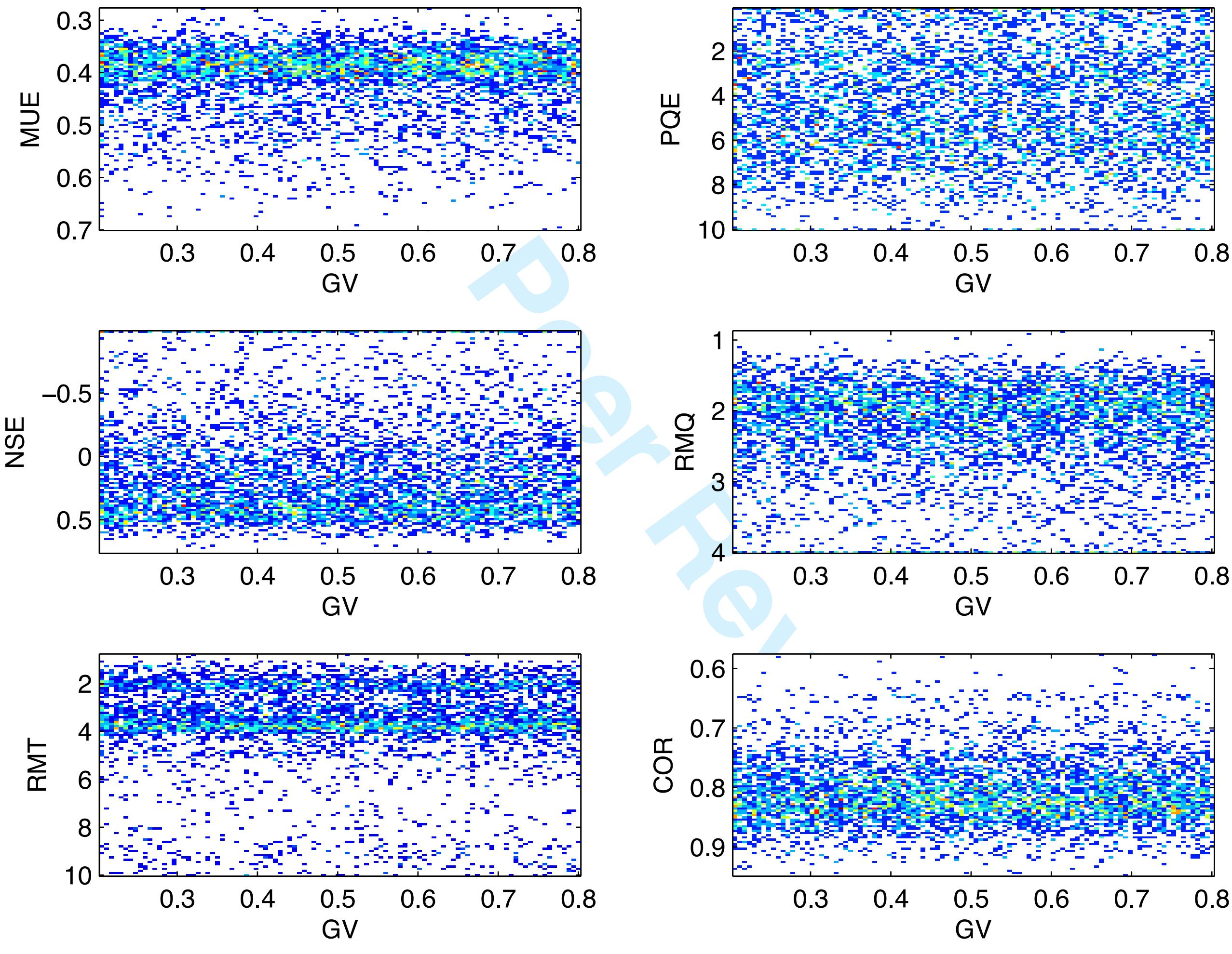
MUE
0.3
0.4
0.5
0.6
0.7
PQE
2
4
6
8
10
NSE
−0.5
0
0.5
RMQ
1
2
3
4
RMT
2
4
6
8
10
COR
0.6
0.7
0.8
0.9
0.3 0.4 0.5 0.6 0.7 0.8
GV

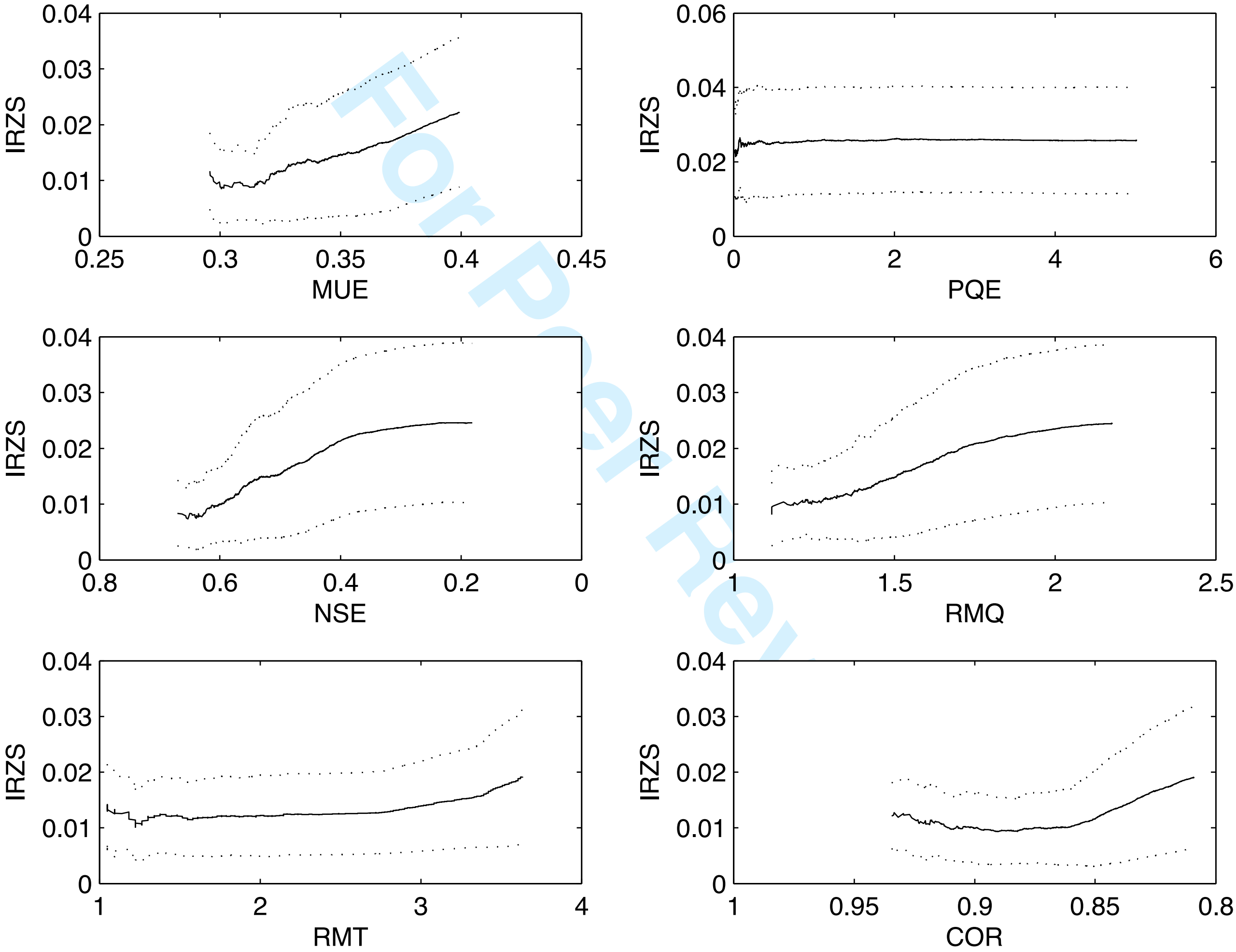
IRZS
MUE
PQE
NSE
RMQ
RMT
COR

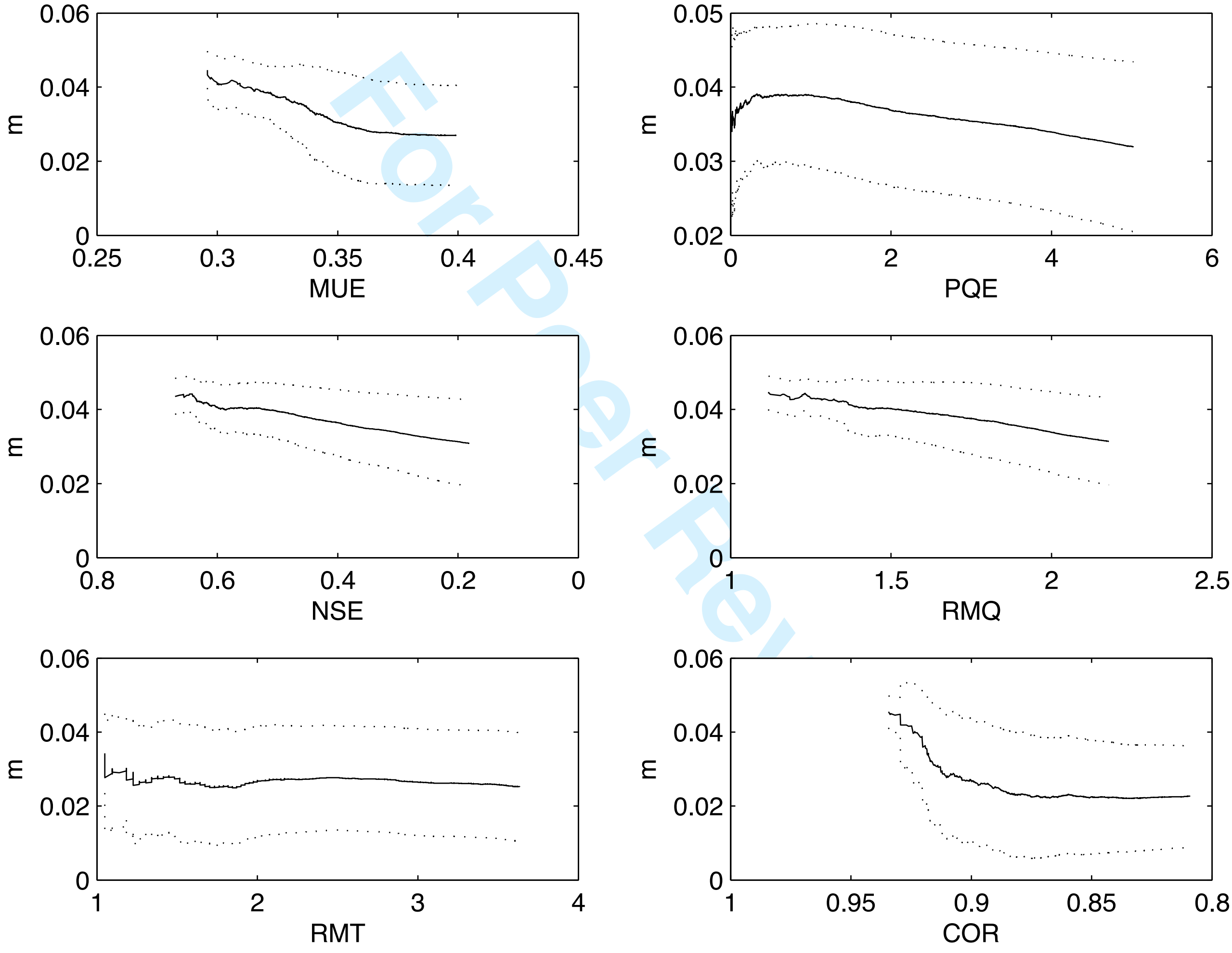
m
MUE
PQE
NSE
RMQ
RMT
COR

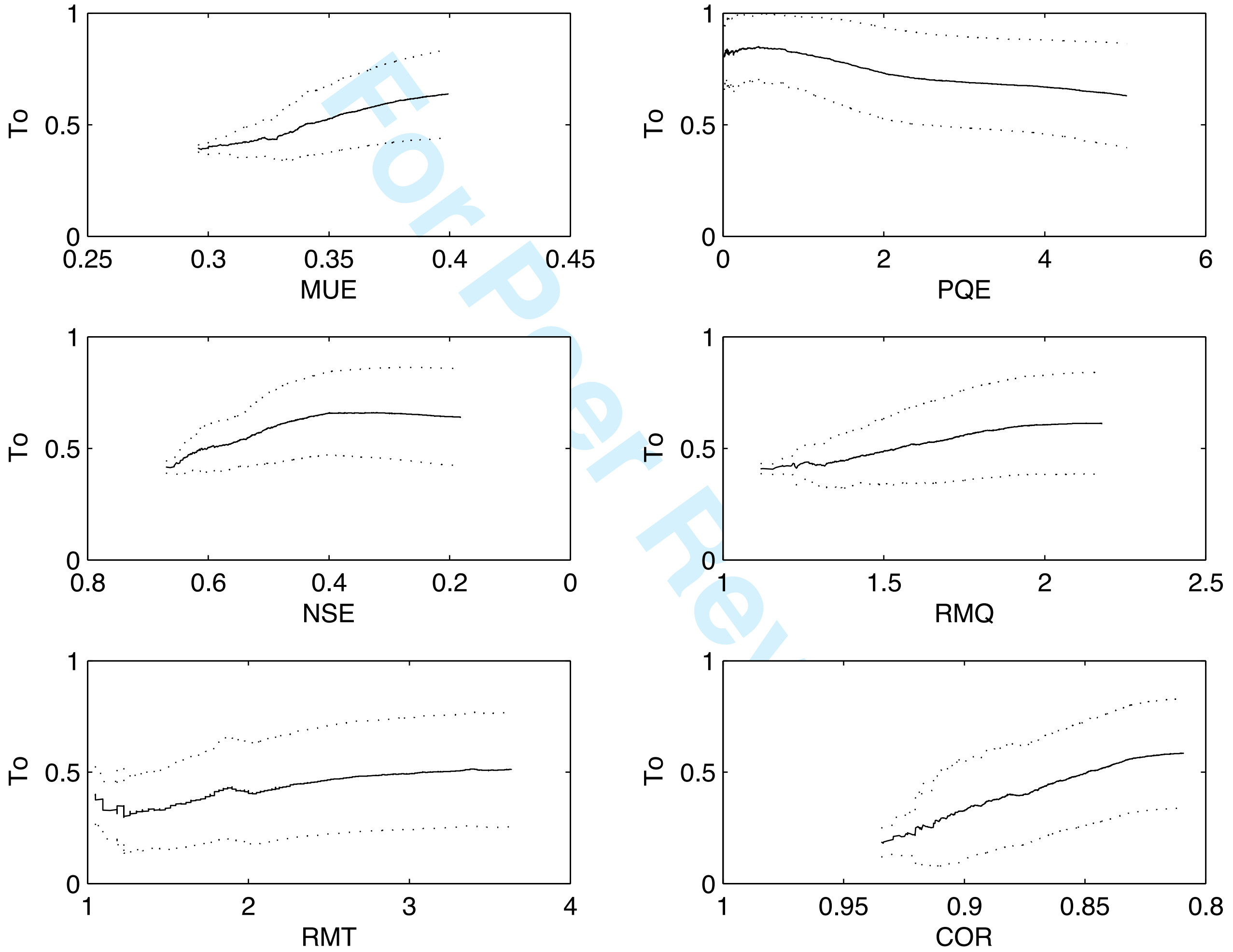
To
MUE
PQE
NSE
RMQ
RMT
COR
0
0.5
1
0.25
0.3
0.35
0.4
0.45
2
4
6
0.8
0.6
0.2
1.5
2.5
3
0.95
0.9
0.85

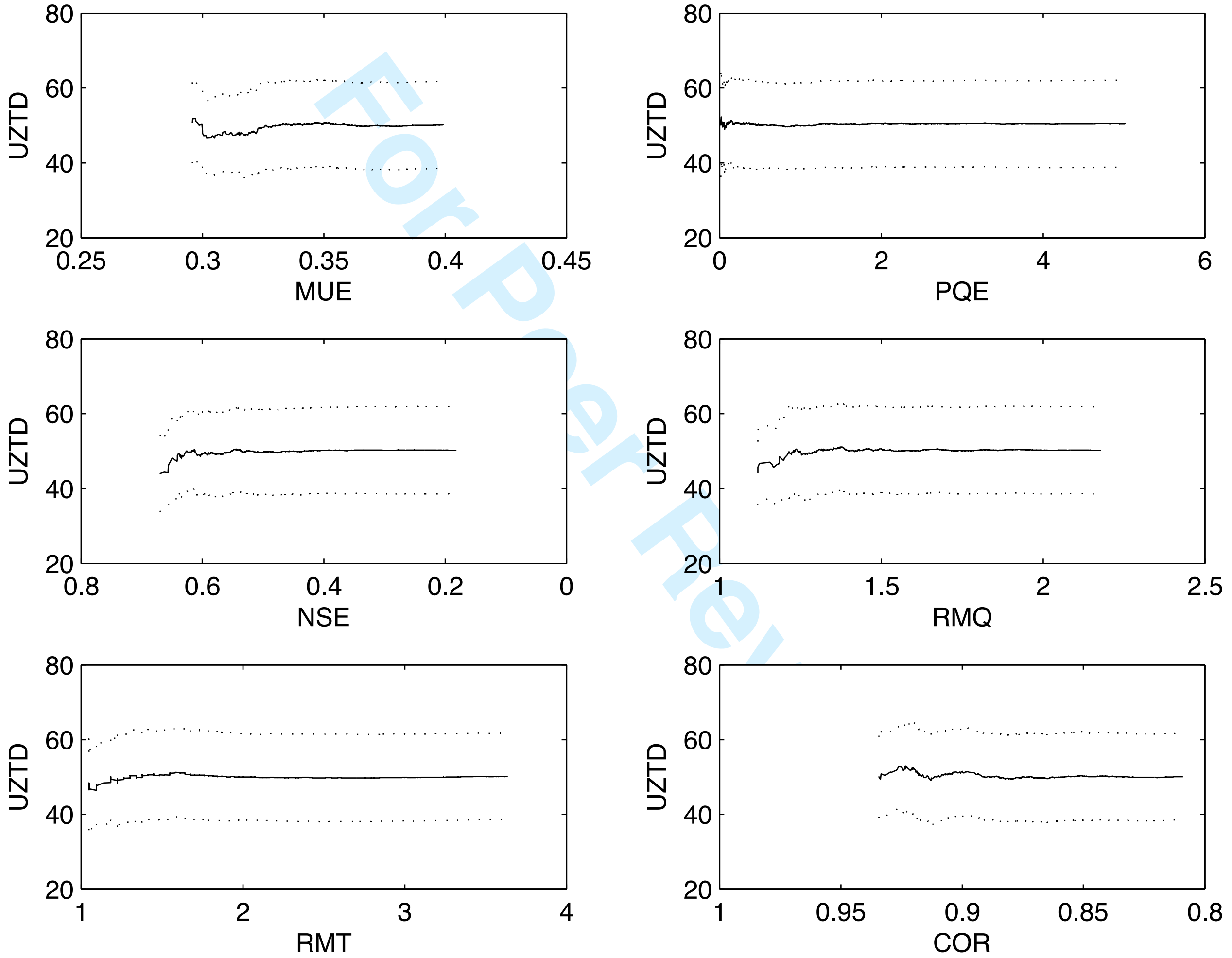
UZTD
MUE
PQE
NSE
RMQ
RMT
COR

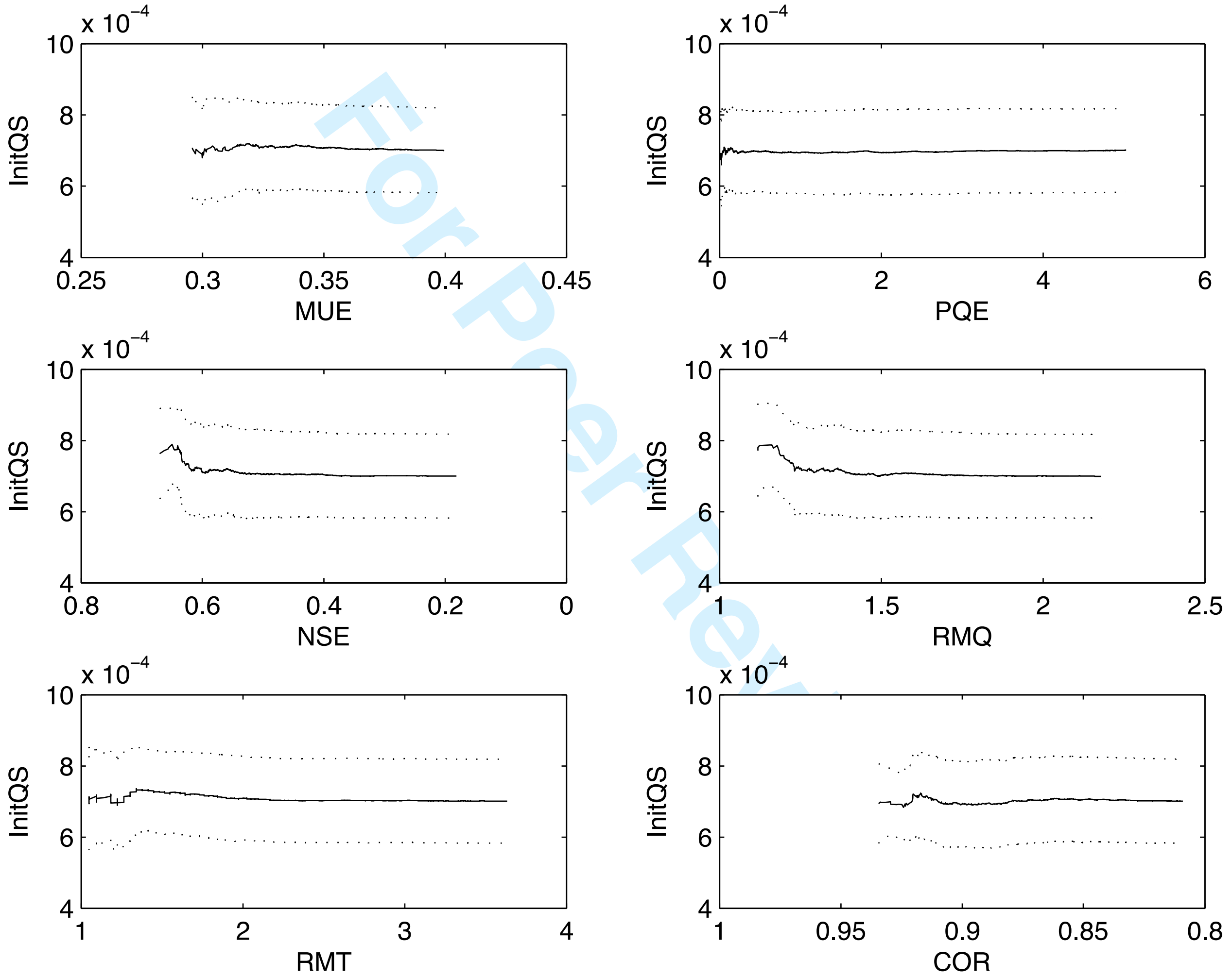
x 10^-4
InitQS
MUE
PQE
NSE
RMQ
RMT
COR

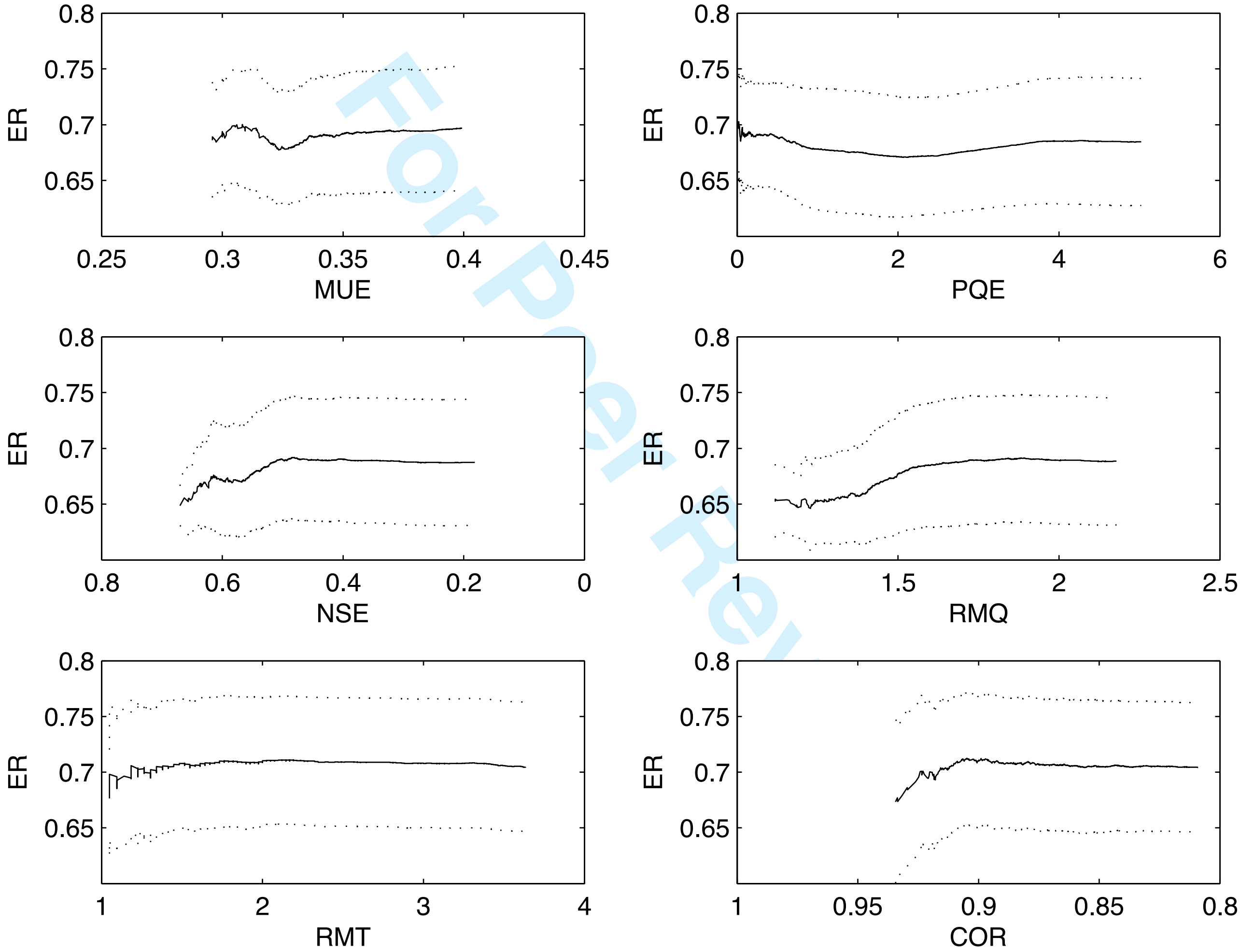

ER
MUE
0.25
0.3
0.35
0.4
0.45
0.8
0.75
0.7
0.65
PQE
0
2
4
6
NSE
0.8
0.6
0.4
0.2
0
RMQ
1
1.5
2
2.5
RMT
1
2
3
4
COR
1
0.95
0.9
0.85
0.8

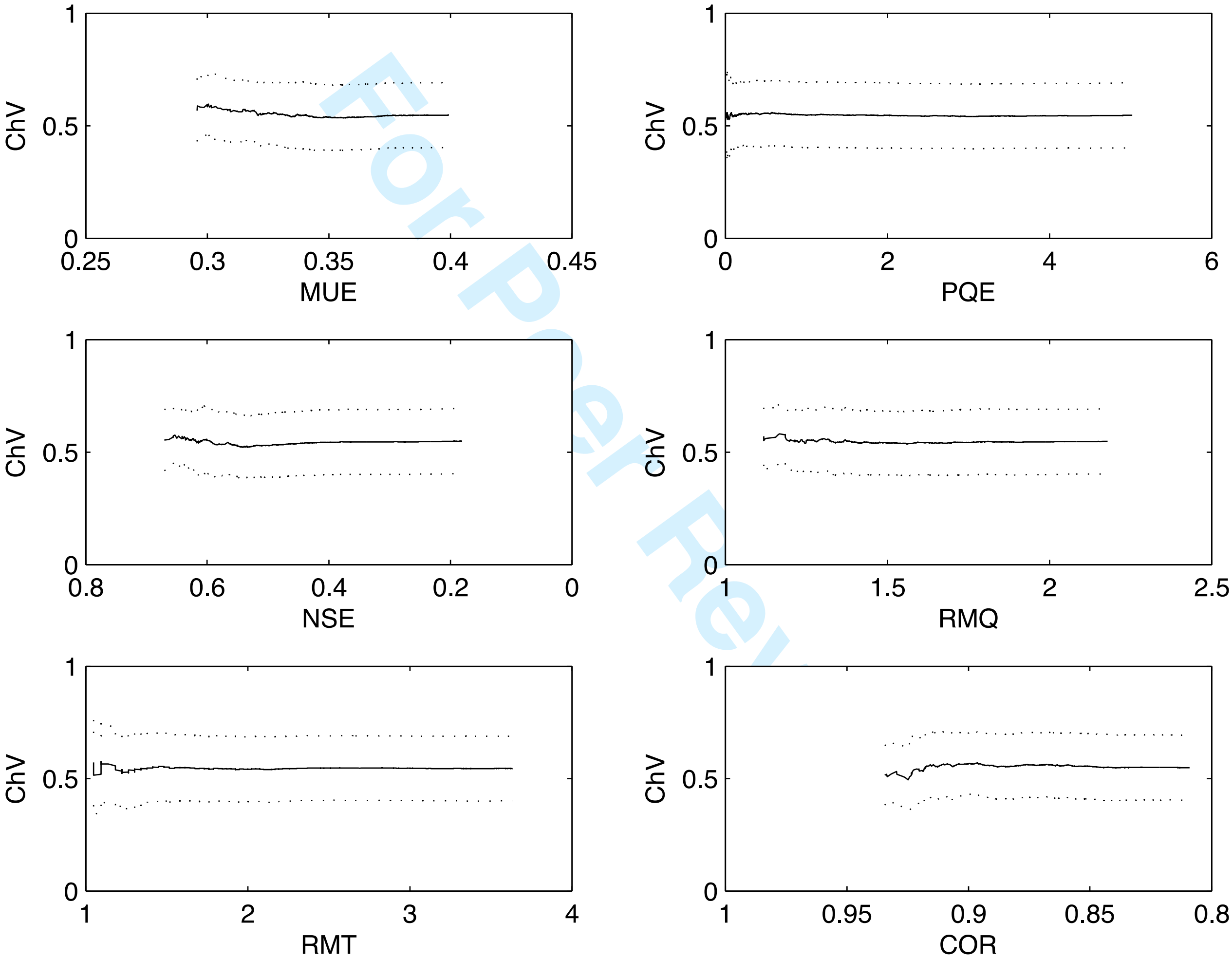
ChV
MUE
0.25
0.3
0.35
0.4
0.45
ChV
PQE
ChV
NSE
ChV
RMQ
ChV
RMT
ChV
COR

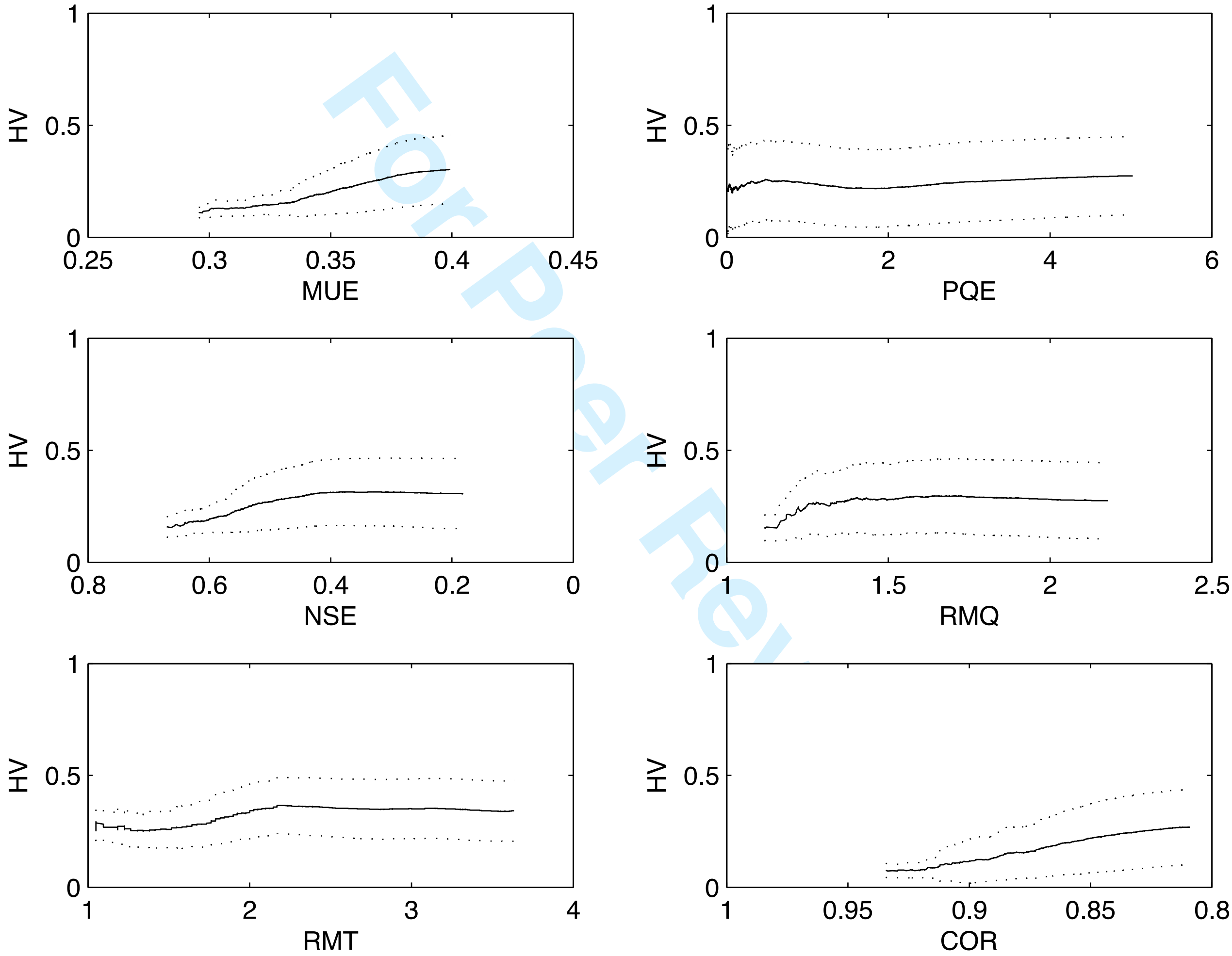
HV
MUE
PQE
NSE
RMQ
RMT
COR

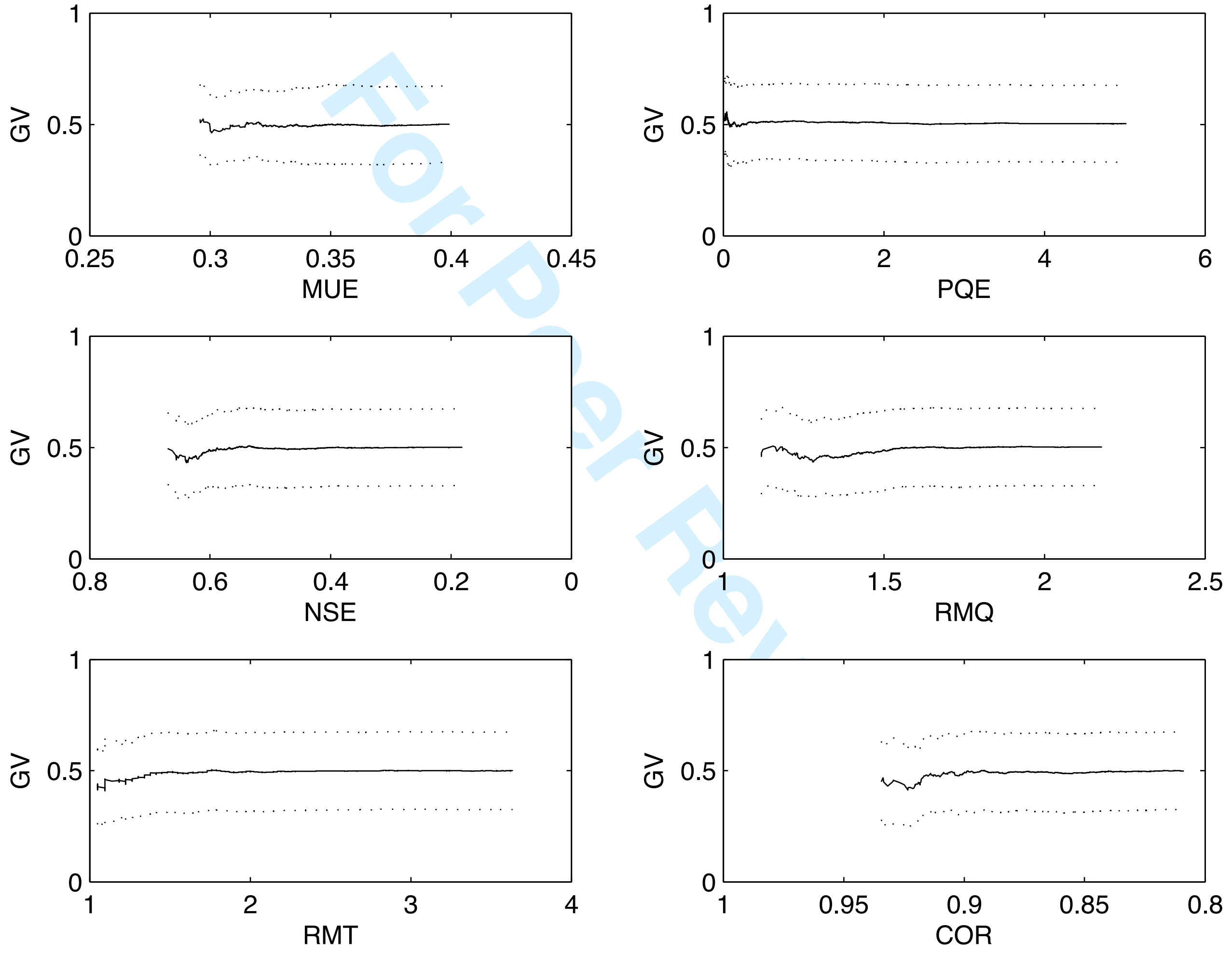
GV
MUE
PQE
NSE
RMQ
RMT
COR
0
0.5
1
0.25
0.3
0.35
0.4
0.45
2
4
6
0.8
0.6
0.2
1.5
2.5
3
0.95
0.9
0.85

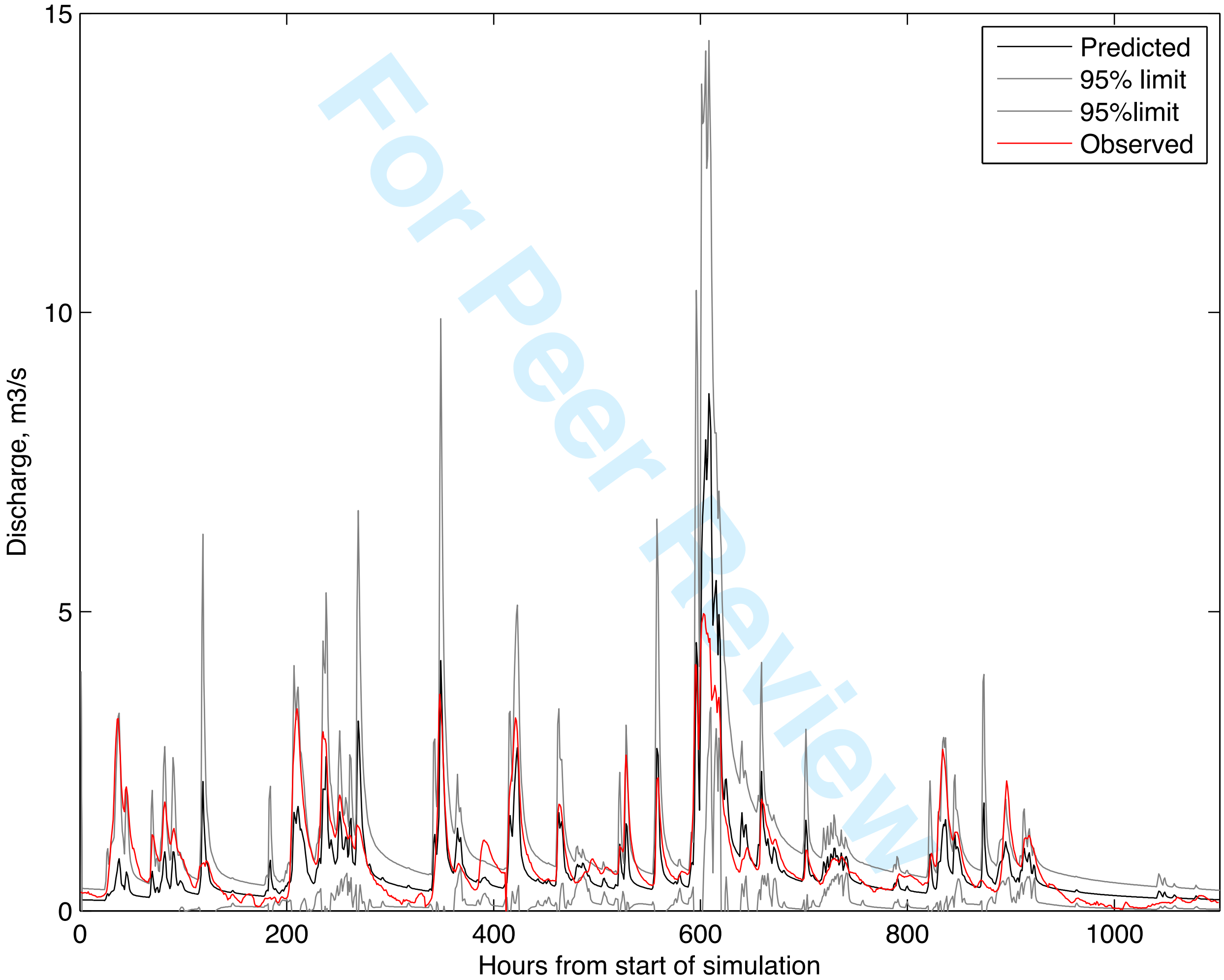
Predicted
95% limit
95%limit
Observed
Discharge, m3/s
Hours from start of simulation
0
5
10
15
0
200
400
600
800
1000

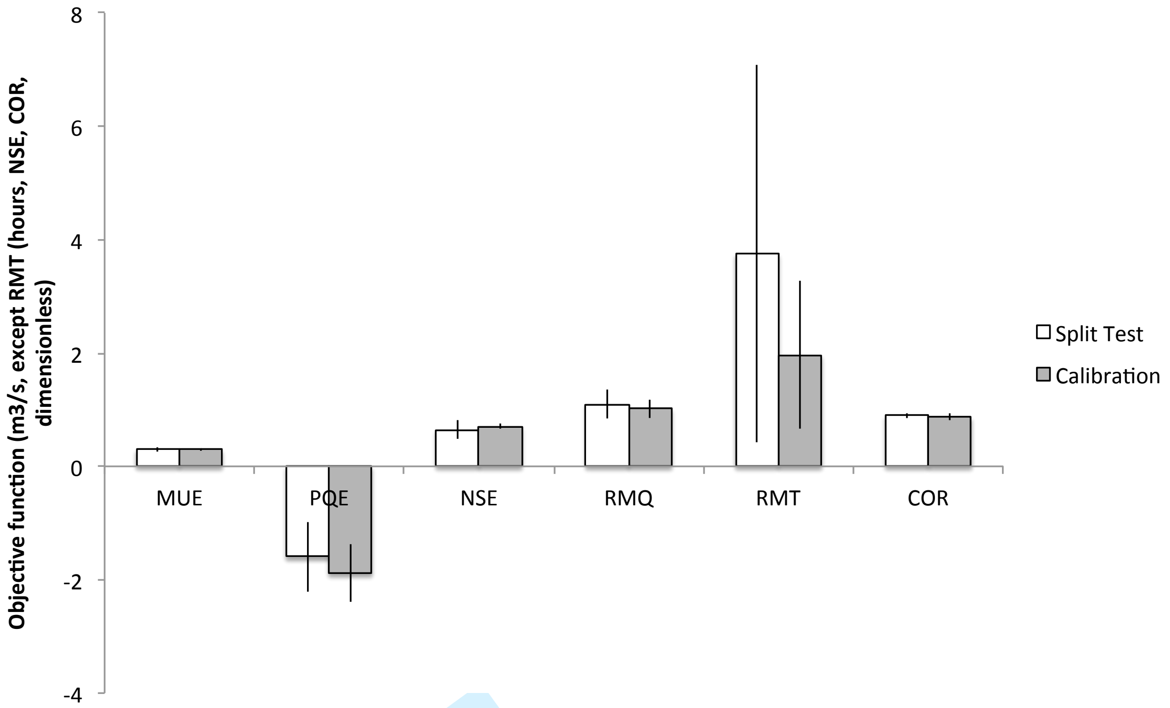
8
6
4
2
0
-2
-4
Objective function (m3/s, except RMT (hours, NSE, COR, dimensionless)
MUE
PQE
NSE
RMQ
RMT
COR
Split Test
Calibration

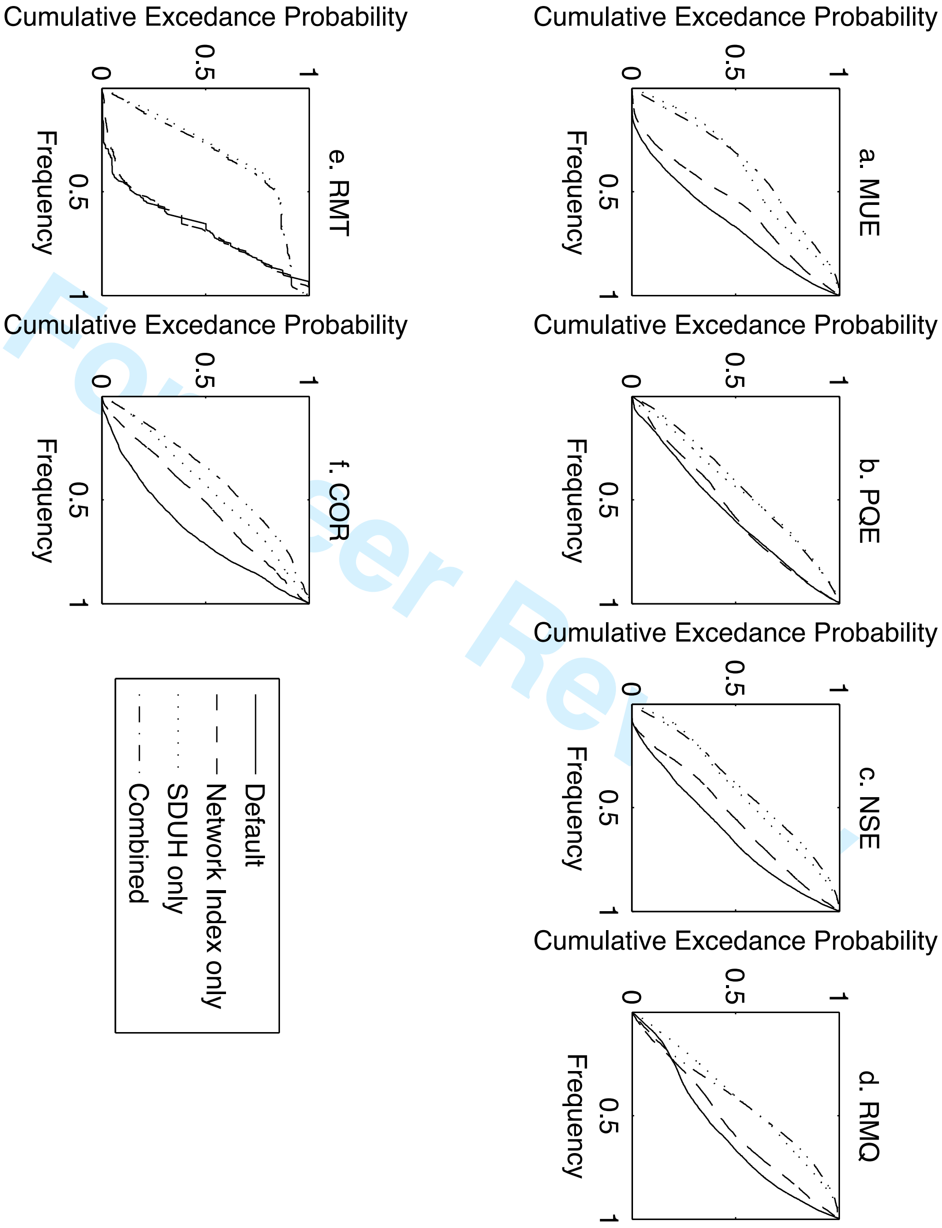
a. MUE
b. PQE
c. NSE
d. RMQ
e. RMT
f. COR
Cumulative Excedance Probability
Frequency
0
0.5
1
Default
Network Index only
SDUH only
Combined

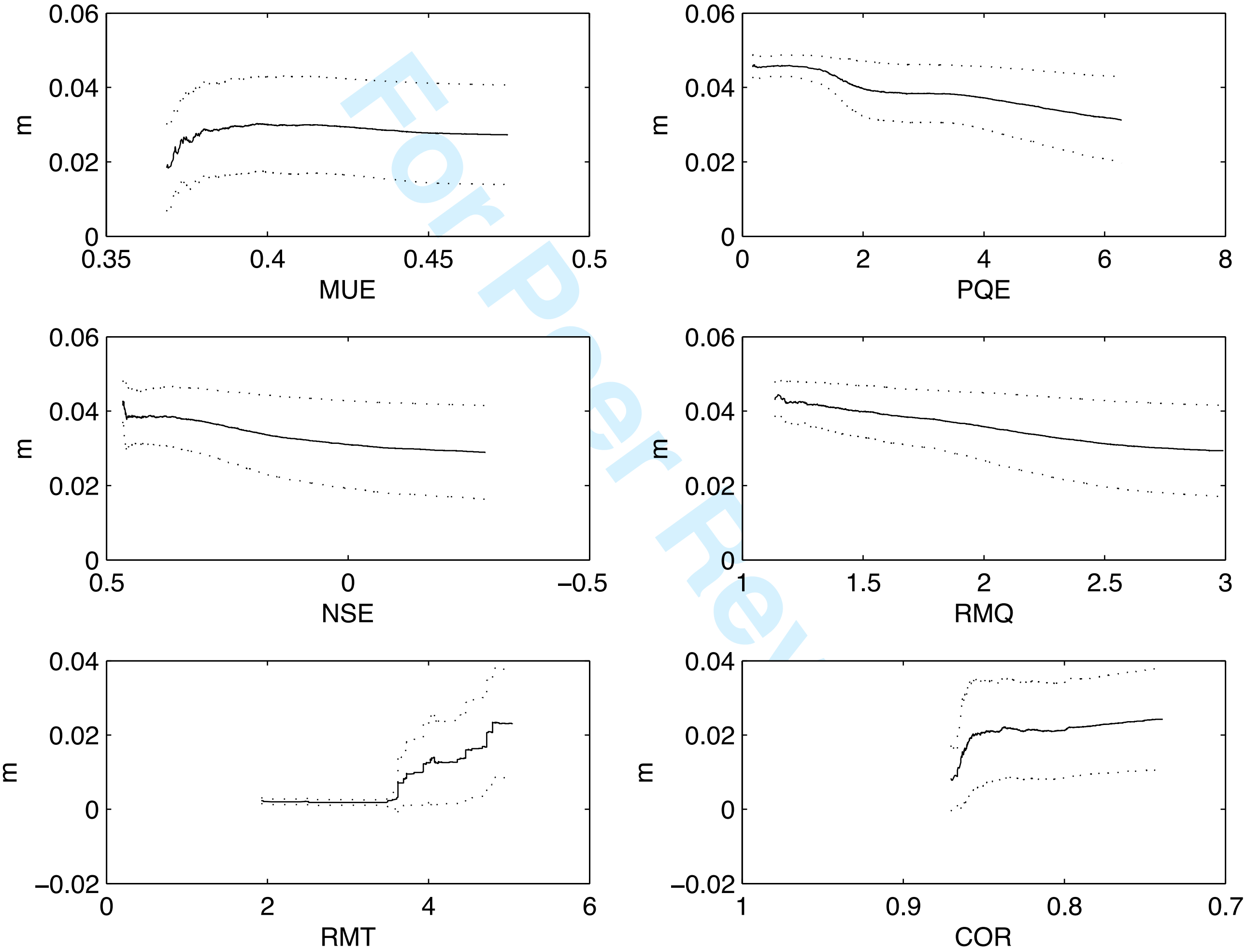

m
MUE
PQE
NSE
RMQ
RMT
COR
0.06
0.04
0.02
0
−0.02
0.35
0.4
0.45
0.5
2
4
6
8
0.5
−0.5
1
1.5
2.5
3
0.9
0.8
0.7

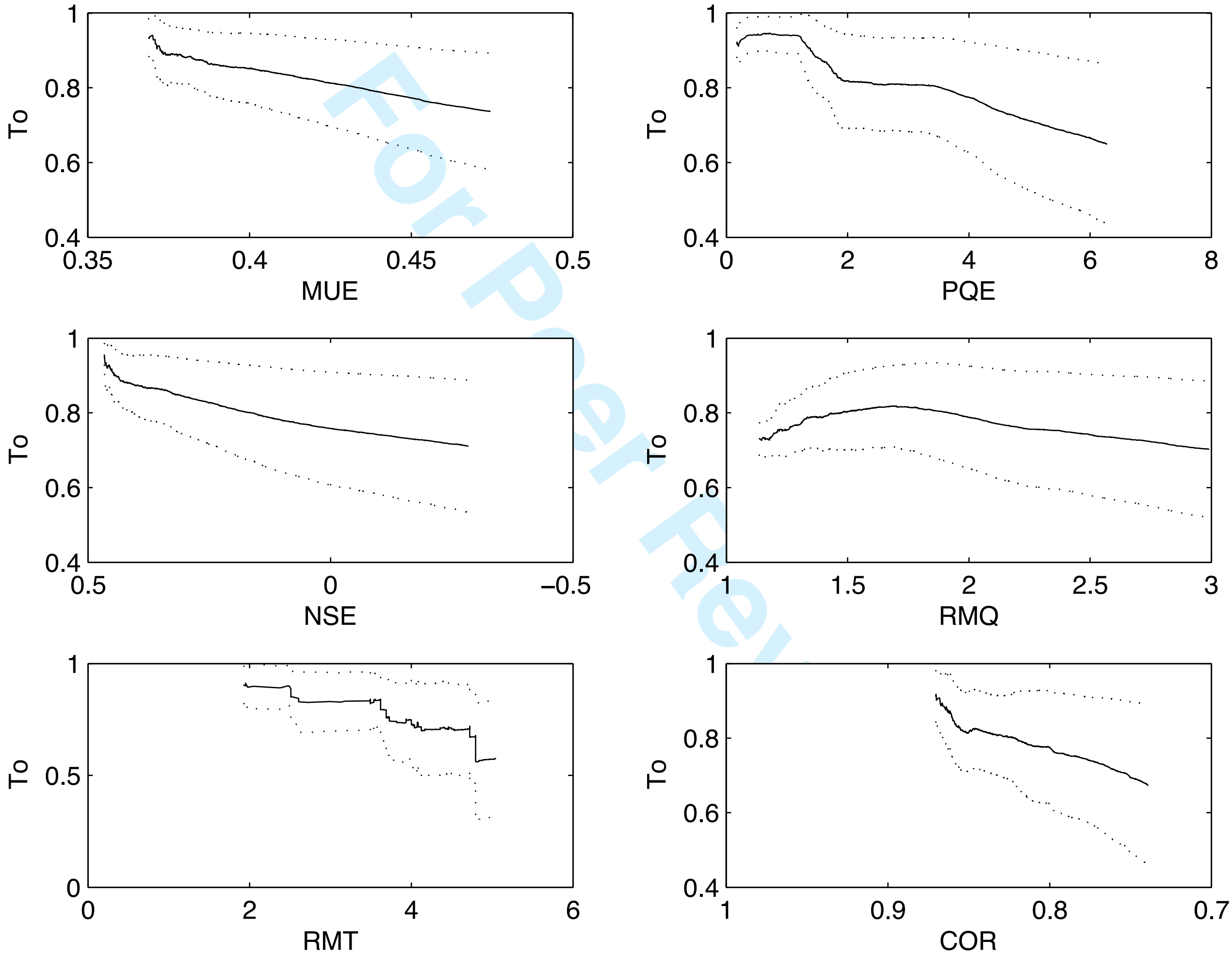
To
MUE
To
PQE
To
NSE
To
RMQ
To
RMT
To
COR

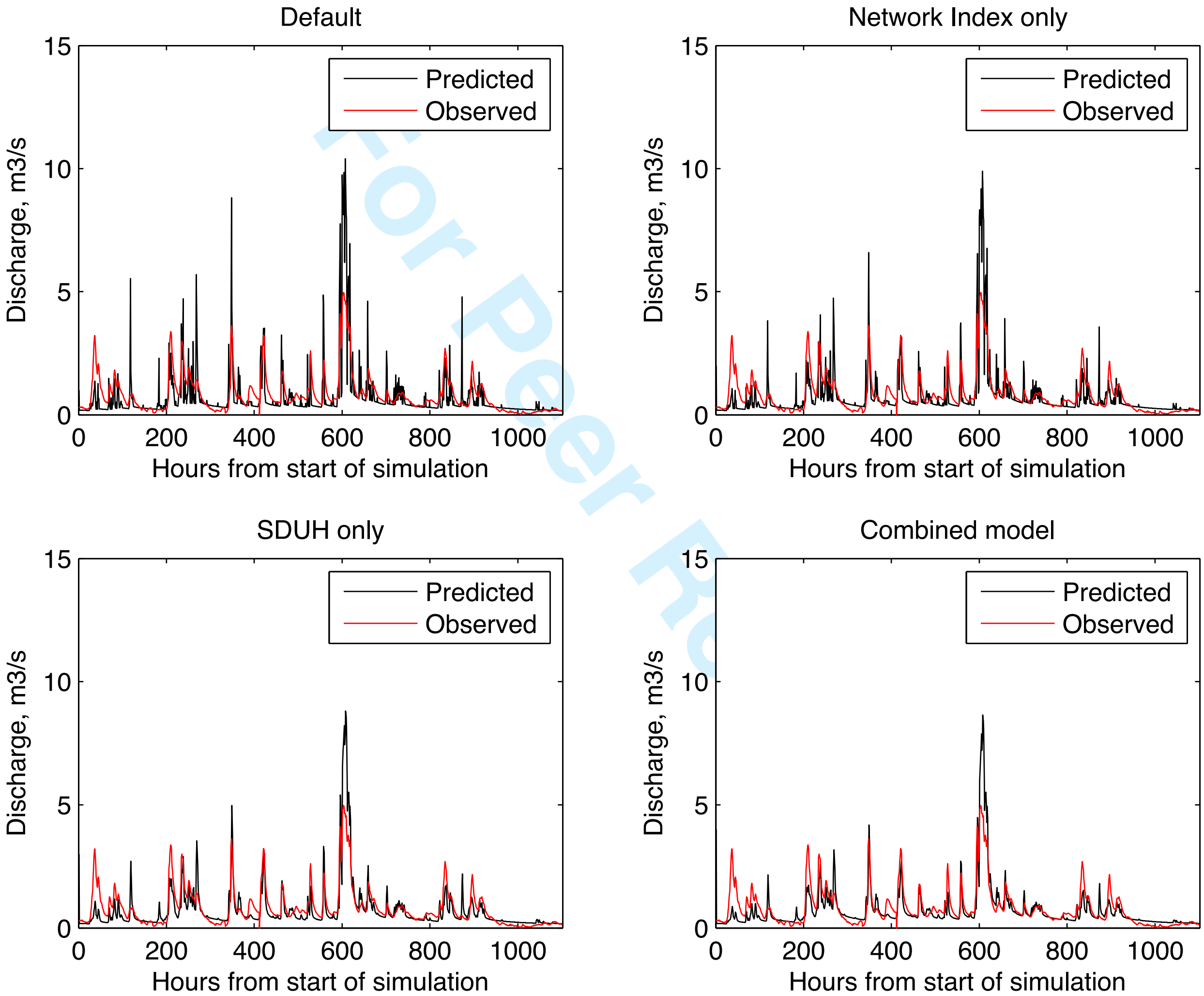

Default
Network Index only
SDUH only
Combined model
Predicted
Observed
Discharge, m3/s
Hours from start of simulation
0
5
10
15
0
200
400
600
800
1000

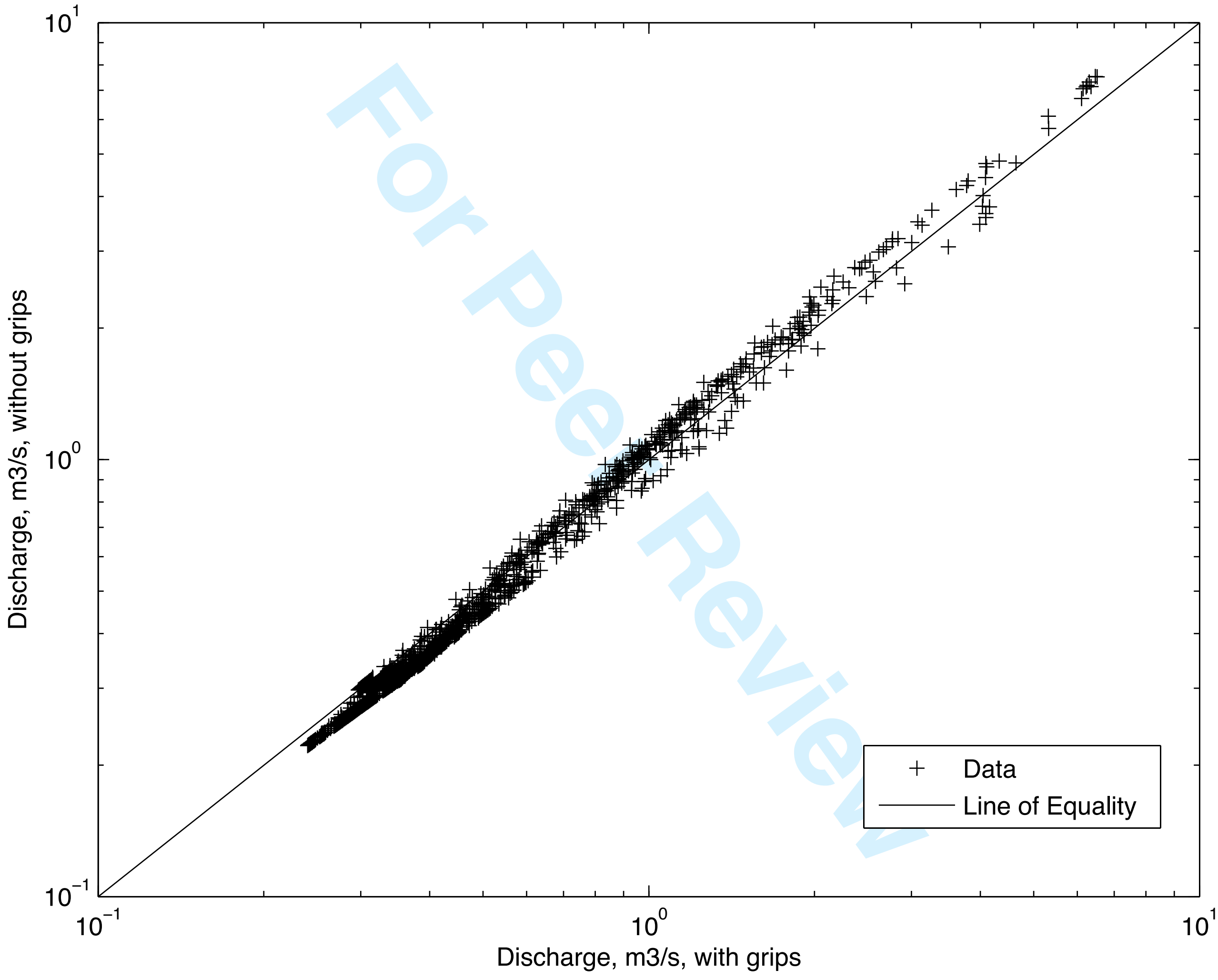
10^{1}
10^{0}
10^{-1}
Discharge, m3/s, without grips
10^{-1}
10^{0}
10^{1}
Discharge, m3/s, with grips
Data
Line of Equality

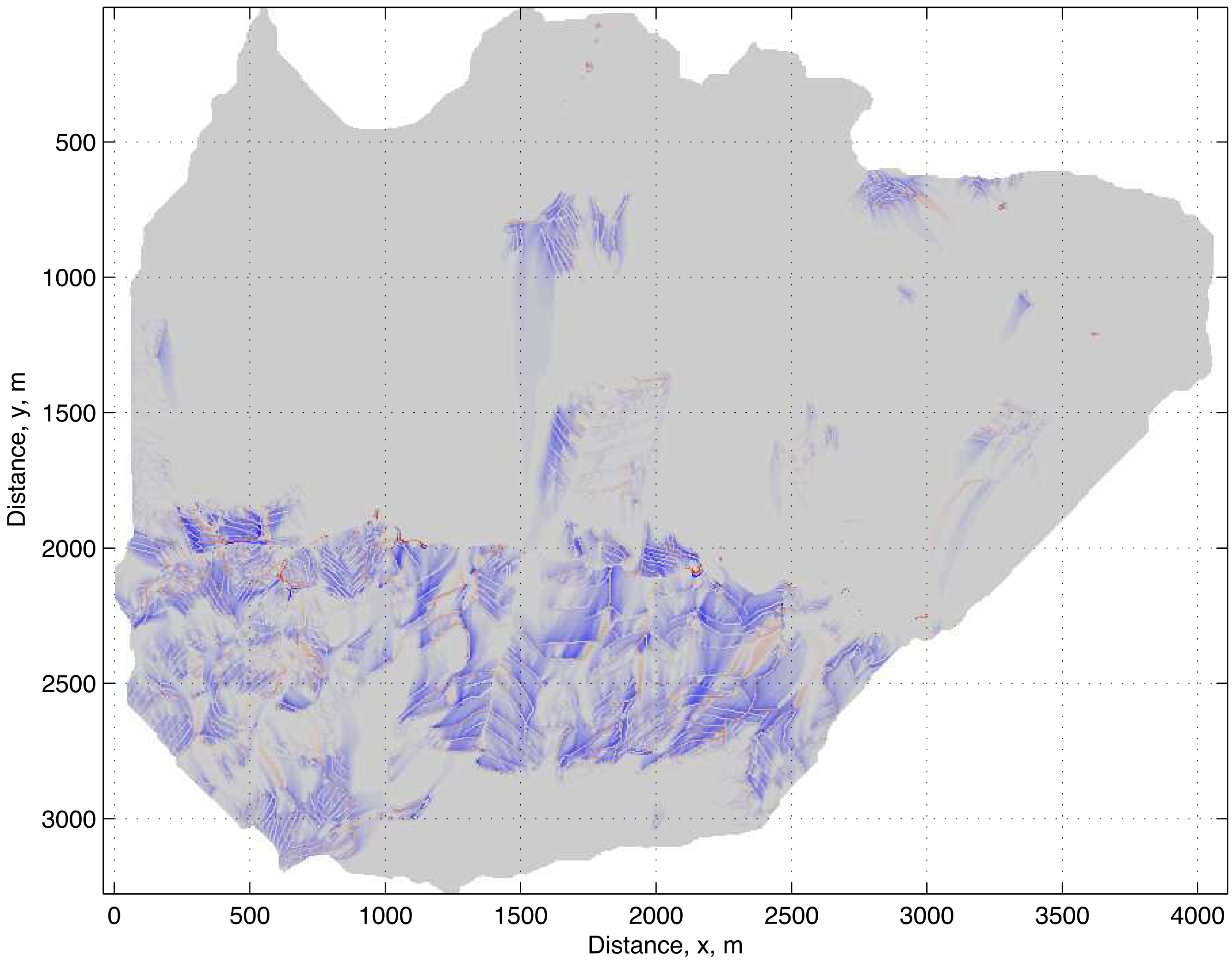

500
1000
1500
2000
2500
3000
Distance, y, m
0
500
1000
1500
2000
2500
3000
3500
4000
Distance, x, m

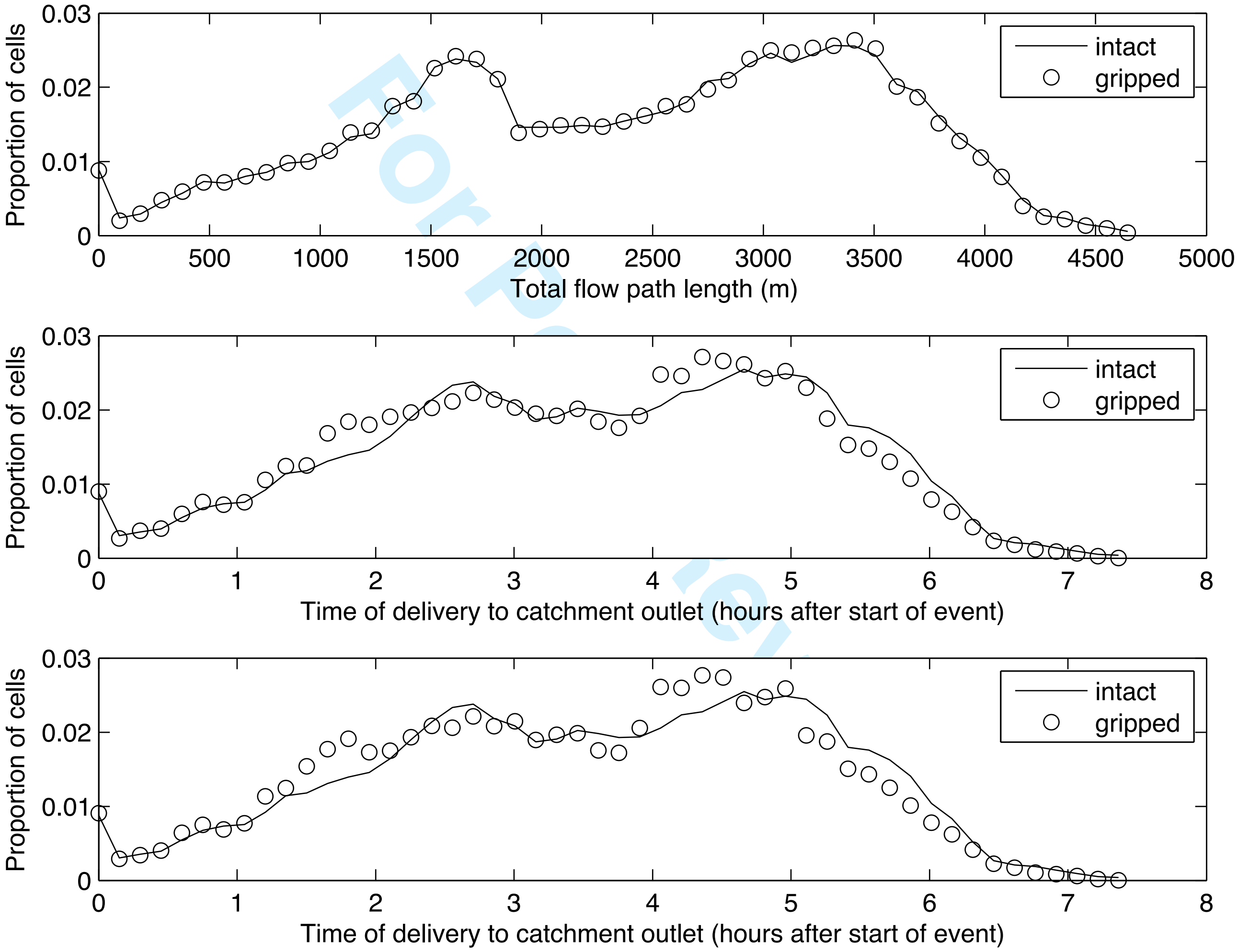
Proportion of cells
0.03
0.02
0.01
0
0
500
1000
1500
2000
2500
3000
3500
4000
4500
5000
Total flow path length (m)
intact
gripped
Proportion of cells
0
1
2
3
4
5
6
7
8
Time of delivery to catchment outlet (hours after start of event)
intact
gripped
Proportion of cells
Time of delivery to catchment outlet (hours after start of event)
intact
gripped

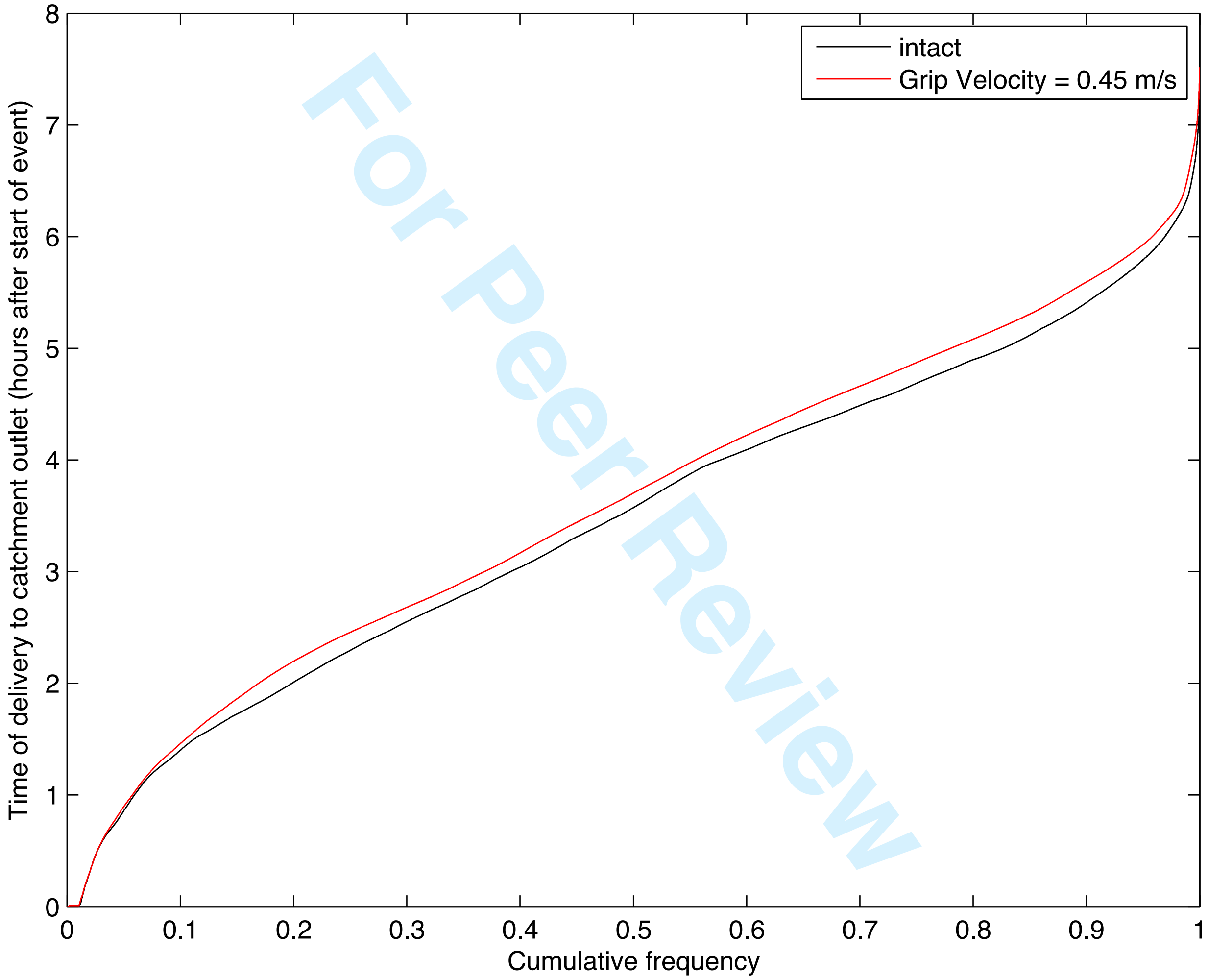
intact
Grip Velocity = 0.45 m/s
Time of delivery to catchment outlet (hours after start of event)
Cumulative frequency
0
1
2
3
4
5
6
7
8
0.1
0.2
0.3
0.4
0.5
0.6
0.7
0.8
0.9

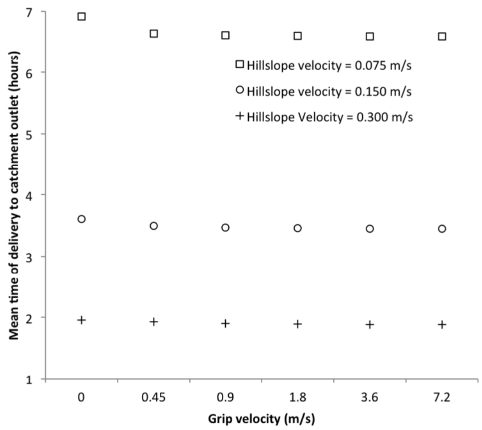

624x468mm (72 x 72 DPI)

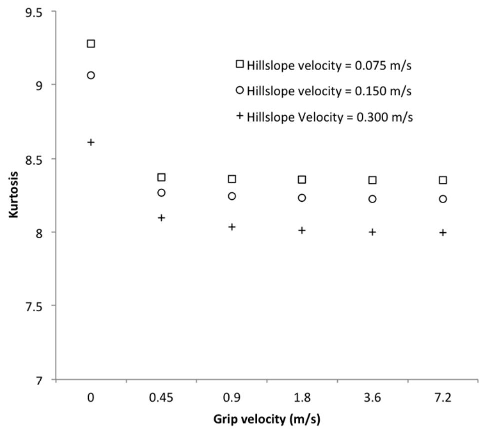

624x468mm (72 x 72 DPI)

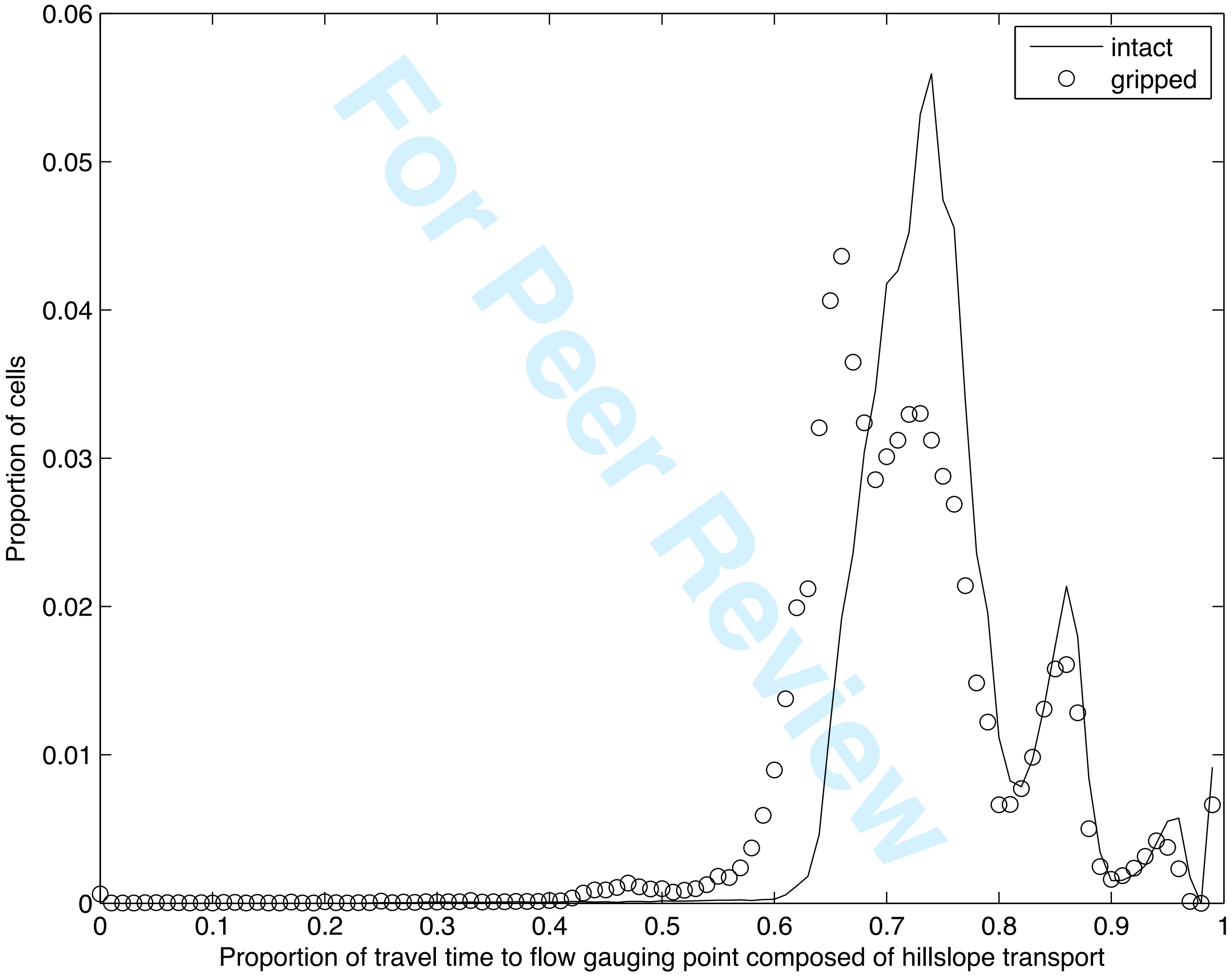
0.06
0.05
0.04
0.03
0.02
0.01
0
Proportion of cells
0
0.1
0.2
0.3
0.4
0.5
0.6
0.7
0.8
0.9
1
Proportion of travel time to flow gauging point composed of hillslope transport
intact
gripped